



Fundação
para a Ciência
e a Tecnologia



LABORATÓRIO DE INSTRUMENTAÇÃO
E FÍSICA EXPERIMENTAL DE PARTÍCULAS

BFKL and low- x physics

Lecture 4

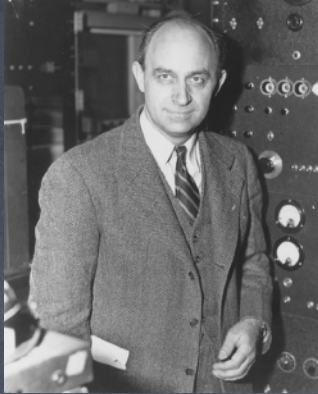
(29-06-2024)

Grigorios Chachamis, LIP Lisbon

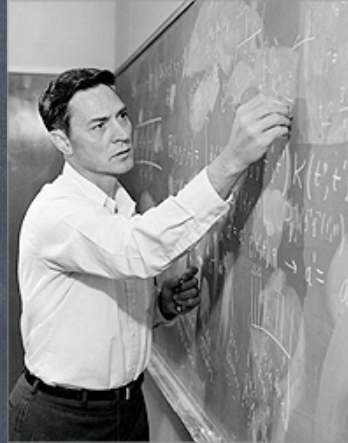
Midsummer School in QCD 2024
Saariselkä, 24 June to 6 July 2024, Finland

Multiperipheral models, S-Matrix, Regge Theory, Bootstrap

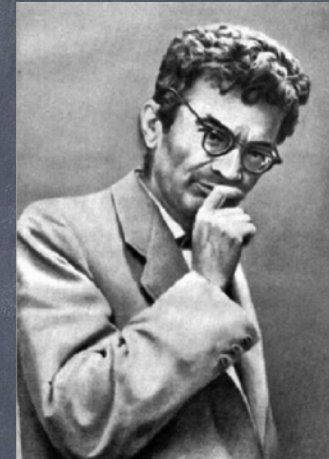
Enrico Fermi
1901-1954



Geoffrey Chew
1924-2019



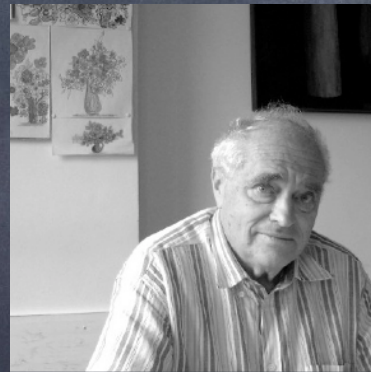
Isaac Pomeranchuk
1913-1966



Sergio Fubini
1928-2005



Daniele Amati
1931



Rolf Hagedorn
1919-2003



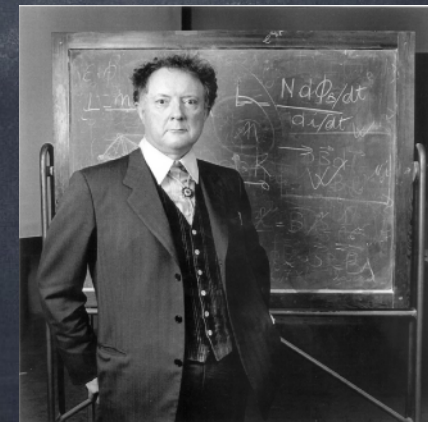
Vladimir Gribov
1930-1997



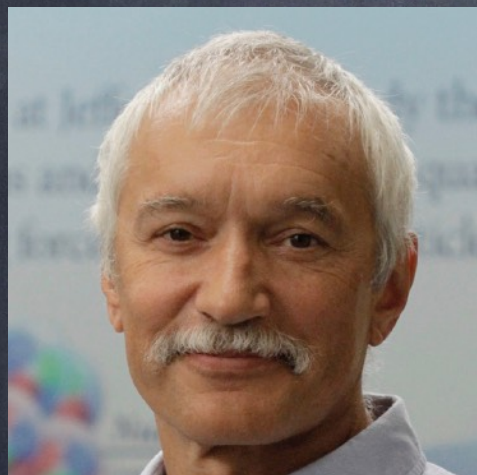
Antonio Stanghellini
1931-1964



Tullio Regge
1931-2014



Balitsky-Fadin-Kuraev-Lipatov



Quantum Chromodynamics

Perturbative and Nonperturbative Aspects

B. L. IOFFE, V. S. FADIN
AND L. N. LIPATOV

CAMBRIDGE MONOGRAPHS
ON PARTICLE PHYSICS, NUCLEAR PHYSICS
AND COSMOLOGY

30

QCD and Collider Physics

R.K. ELLIS, W.J. STIRLING
AND B.R. WEBBER

CAMBRIDGE MONOGRAPHS
ON PARTICLE PHYSICS, NUCLEAR PHYSICS
AND COSMOLOGY

8

V. Barone
E. Predazzi

High-Energy Particle Diffraction

 Springer

Basics of PERTURBATIVE QCD

Yu. L. Dokshitzer, V. A. Khoze
A. H. Mueller and S. I. Troyan



EDITIONS
FRONTIERES

Foundations of Perturbative QCD

JOHN COLLINS

CAMBRIDGE MONOGRAPHS
ON PARTICLE PHYSICS, NUCLEAR PHYSICS
AND COSMOLOGY





32

Quantum Chromodynamics and the Pomeron


CAMBRIDGE
LECTURE
NOTES IN
PHYSICS

J. R. FORSHAW
& D. A. ROSS

Evolution equations in the low x regime

- Balitsky-Fadin-Kuraev-Lipatov (BFKL)  linear
- Gribov-Levin-Ryskin Mueller-Qiu (GLR-MQ)  non-linear
- Ciafaloni-Catani-Fiorani-Marchesini (CCFM)
- Balitsky-Kovchegov (BK)  non-linear
- Jalilian Marian-Iancu-MacLerran-Weigert-Leonidov-Kovner (JIMWLK)  non-linear
- Various "improved" versions

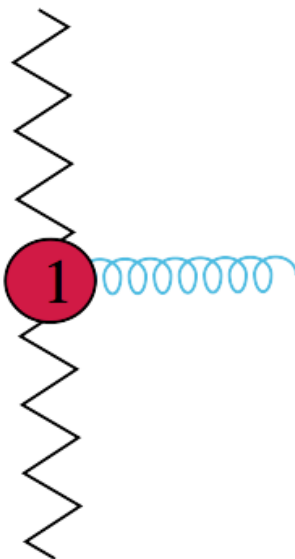
BFKL equation to higher orders

- We have seen the BFKL equation "derived" to leading logarithmic accuracy (LLA)
- The resummation of large logarithms (numerically large) was done by taking into account all terms of the form $(\alpha_s \ln s)^n$ (LLA)
- When we resum the next large logarithms (NLLA), we consider the Feynman diagrams that contribute term of the form $\alpha_s (\alpha_s \ln s)^n$. Corrections large!!
- What about the NNLLA BFKL?

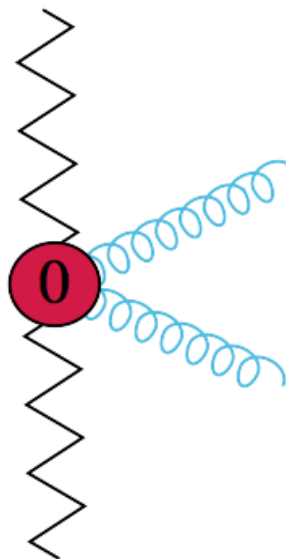
NLO BFKL



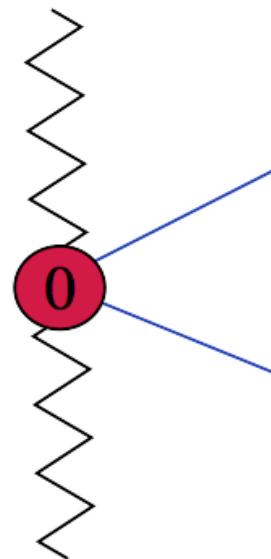
2-loop trajectory



1-loop g emission



pair production



Where to look for BFKL related effects

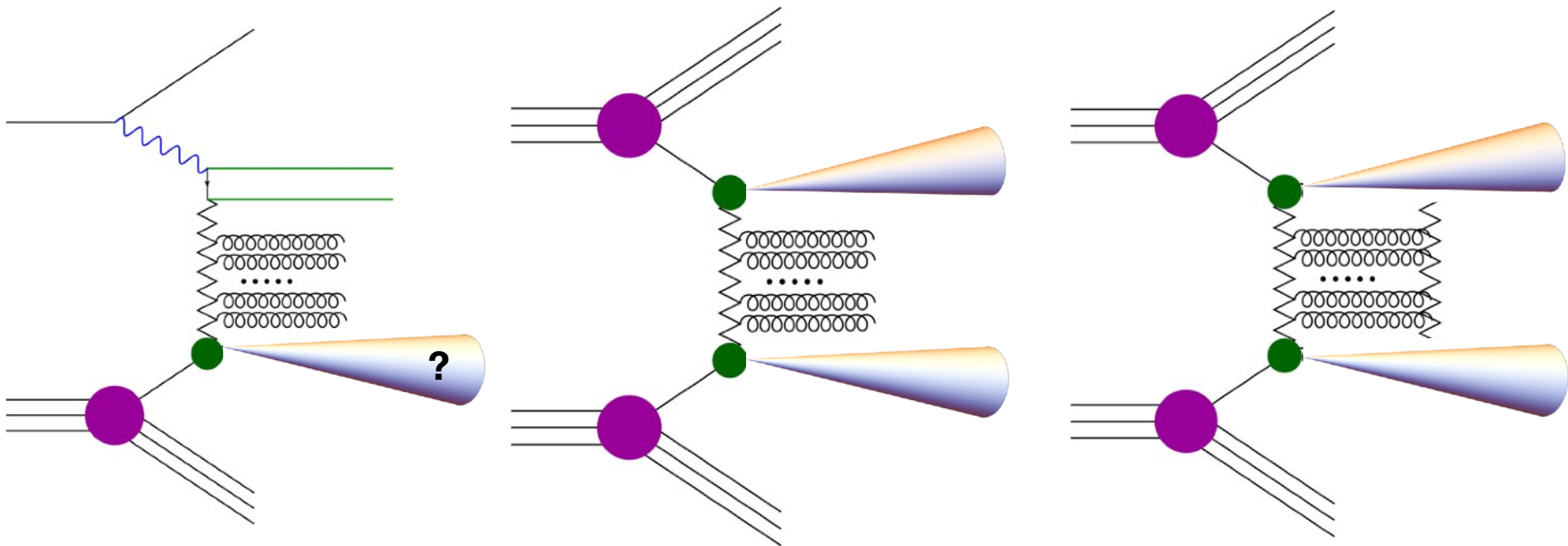
BFKL applicable in various scenarios?

1. Deep Inelastic Scattering (DIS)?

2. Production of two hard jets well separated in rapidity?

3. Diffractive events?

Instead of two jets, one may have one jet and one hadron or even two hadrons.



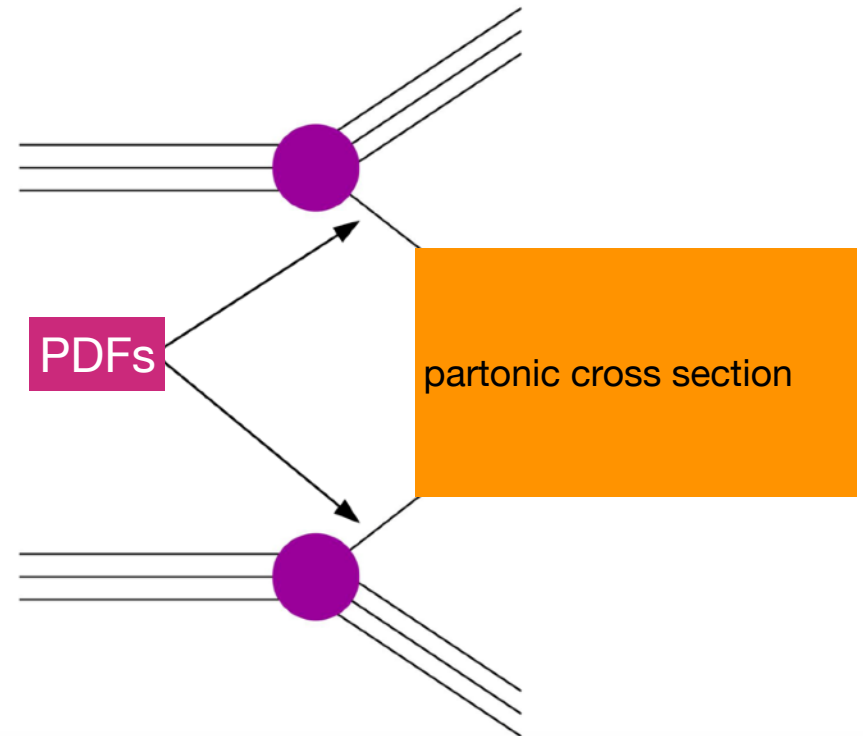
Collinear factorization scheme

Collins Soper Serman 1989

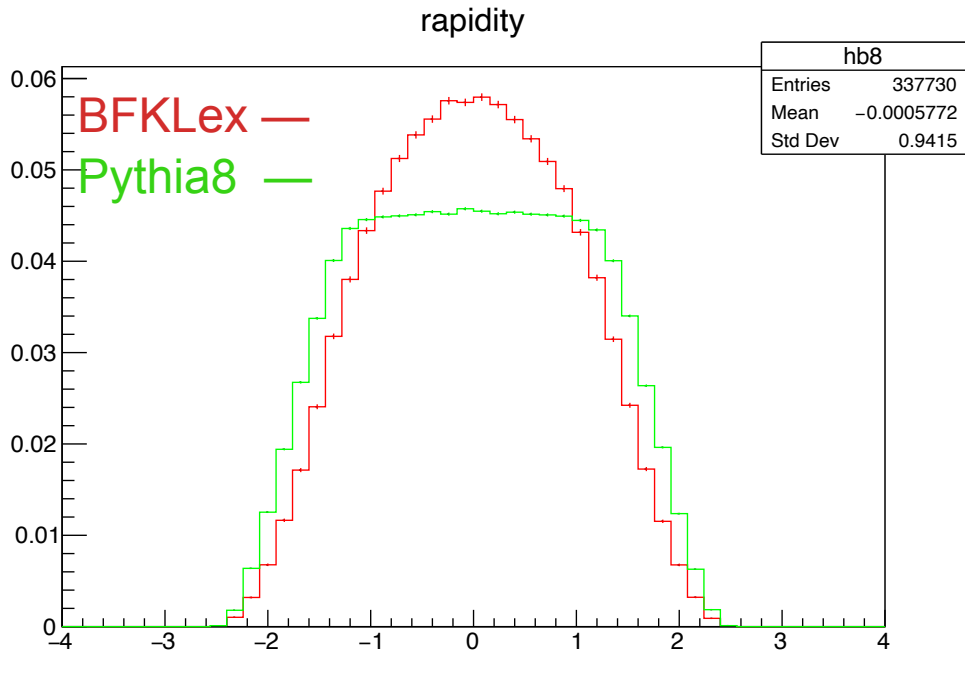
$$\sigma(s) = \sum_{i,j} \int dx_1 dx_2 f_i(x_1) f_j(x_2) \hat{\sigma}_{ij}(x_1 x_2 \hat{s})$$

- The partonic cross section is convoluted with the PDFs

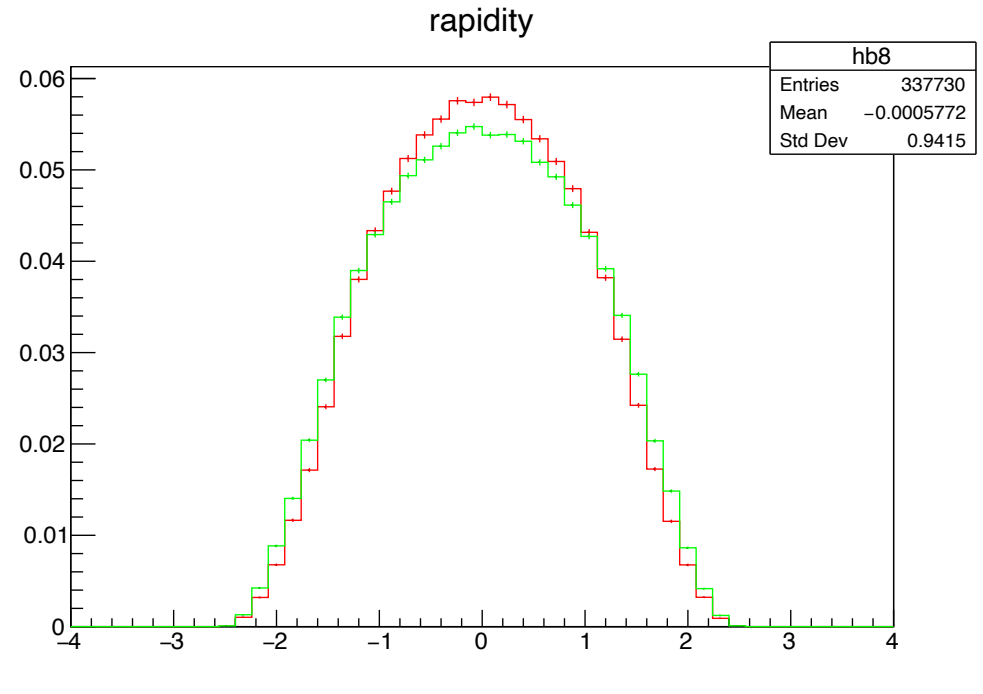
$$\frac{\partial f_i(x, Q^2)}{\partial \log(Q^2)} = \sum_j \int_x^1 \frac{dz}{z} P_{j \rightarrow i}(z) f_j\left(\frac{x}{z}, Q^2\right)$$



what is the difference?

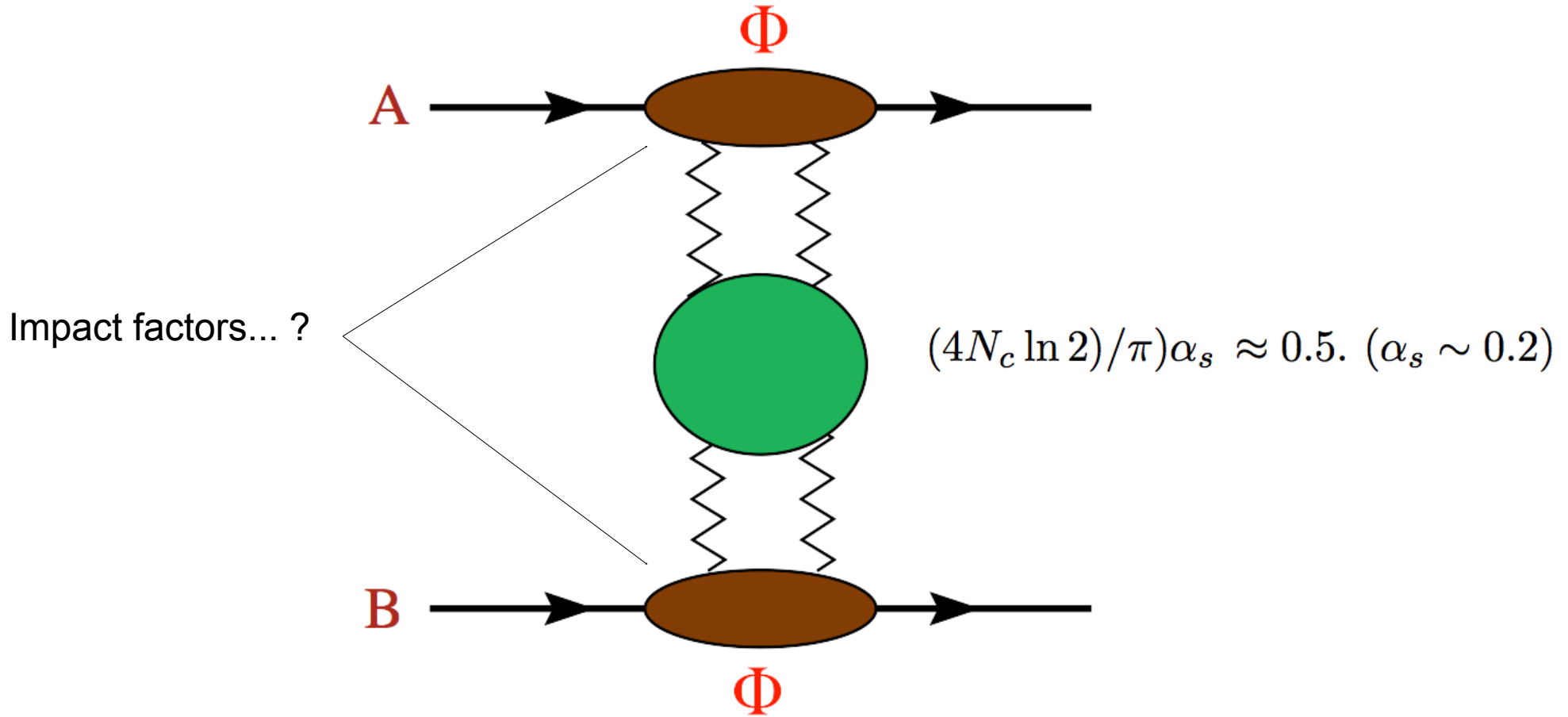


Plot 1



Plot 2

A hadronic elastic amplitude



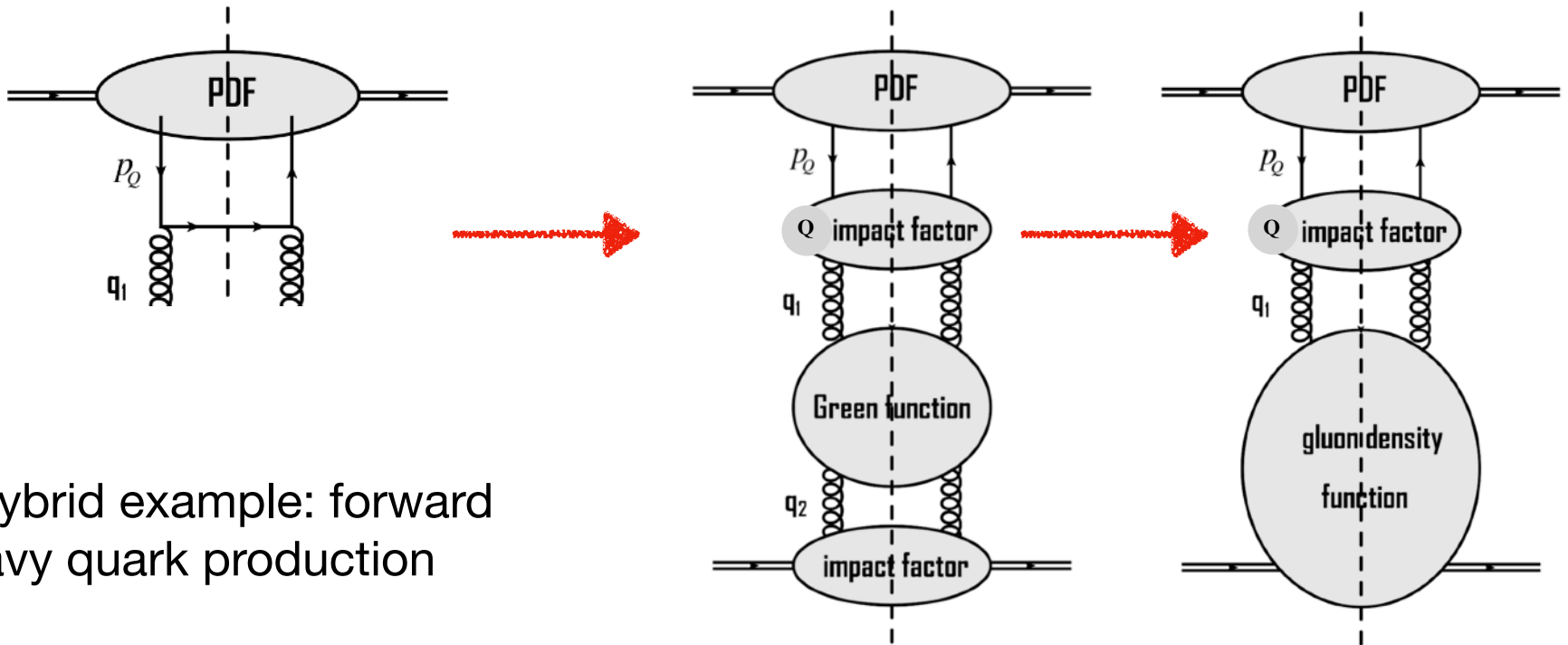
$$\mathcal{A}(s, t) = i s C \int \frac{d^2 \mathbf{k}_1}{(2\pi)^2} \frac{d^2 \mathbf{k}_2}{(2\pi)^2} \Phi_A(\mathbf{k}_1, \mathbf{q}) \frac{f(s, \mathbf{k}_1, \mathbf{k}_2, \mathbf{q})}{\mathbf{k}_2^2 (\mathbf{k}_1 - \mathbf{q})^2} \Phi_B(\mathbf{k}_2, \mathbf{q})$$

Impact factors

- Impact factors are effective couplings of the BFKL gluon Green's function to the colliding projectiles
- They are process dependent objects
- One needs to calculate them at a certain order of the perturbative expansion, preferably the same one as that of the BFKL gluon Green's function.
- It is not an easy task to calculate impact factors to NLO.

k_T -factorization scheme (and hybrids)

$$\sigma(s) = \int \frac{dx_1}{x_1} f_i(x_1) d^2 k_{2\perp} \frac{dx_2}{x_2} \mathcal{F}(x_2, k_{2\perp}) \hat{\sigma}(x_1 x_2 s, k_{1\perp} \rightarrow 0, k_{2\perp})$$



- A hybrid example: forward heavy quark production

BFKL Quiz

1. What does BFKL stand for in the context of QCD?

- A) Balitsky-Fadin-Kuraev-Lipatov
- B) Bose-Fermi-Klein-Landau
- C) Beta-Fermi-Kinetic-Lagrange

2. What is the main focus of the BFKL equation?

- A) Resumming leading logarithms of momentum transfer
- B) Resumming leading logarithms of energy
- C) Calculating fermion masses

3. In which limit of QCD is BFKL primarily applicable?

- A) Low energy

- B) High energy

- C) Intermediate energy

4. What physical phenomenon does the BFKL Pomeron describe?

- A) Particle decay

- B) Rising cross-sections at high energies

- C) Electromagnetic interactions

5. What does the BFKL equation predict about the gluon density at small x ?

- A) Decrease

- B) Constant

- C) Increase

1. What type of interaction is primarily mediated by the BFKL Pomeron?

- A) Strong interaction
- B) Electromagnetic interaction
- C) Weak interaction

2. Which particles are involved in the exchanges described by the BFKL equation?

- A) Photons
- B) Gluons
- C) W and Z bosons

3. What is a key feature of the BFKL equation compared to the DGLAP equations?

- A) It focuses on small x behavior.

- B) It deals with large Q^2 .

- C) It describes heavy quark production.

4. In BFKL physics, what does the term 'reggeization' refer to?

- A) The process of particle decay

- B) The modification of particle trajectories

- C) The quantization of gluon fields

5. What kind of approximation is commonly used in BFKL calculations?

- A) Low-energy approximation

- B) High-energy approximation

- C) Quasi-static approximation

1. What role does the strong coupling constant α_s play in the BFKL equation?

- A) It is negligible.
- B) It appears in the prefactor and affects the trajectory.
- C) It is irrelevant.

2. How does the BFKL approach treat transverse momentum?

- A) Ignores it.
- B) Resums logarithms related to it.
- C) Assumes it is constant.

3. What is the significance of the 'ladder diagrams' in BFKL calculations?

- A) They are used to describe weak interactions.
- B) They represent the exchanged gluons and reggeized gluons.

- C) They describe decay processes.

4. In BFKL physics, what is the 'rapidity gap'?

- A) A region in a detector where no particle production is observed, indicating a color-neutral exchange.
- B) A space where particles are dense for a wide gap
- C) An energy threshold.

5. What impact do higher-order corrections have on BFKL predictions?

- A) No impact.
- B) They refine predictions although they may introduce further uncertainties.
- C) They invalidate the model.

1. What is the connection between BFKL dynamics and the concept of saturation in QCD?

- A) They are unrelated.
- B) BFKL predicts unlimited growth, which saturation counters by balancing gluon density growth.
- C) Saturation decreases gluon density.

2. How do NLLA (Next-to-Leading Logarithmic Approximation) corrections impact BFKL predictions?

- A) They have negligible effect.
- B) They significantly alter the predicted growth rates of cross-sections.
- C) They eliminate all uncertainties.

3. What phenomenon does the BFKL equation fail to account for without saturation effects?

- A) Decrease in energy.

- B) Unbounded increase in gluon density.

- C) Mass of quarks.

4. Why are the NLLA corrections in BFKL considered large and significant?

- A) They only apply at low energies.

- B) They suggest substantial modifications to the leading-order predictions.

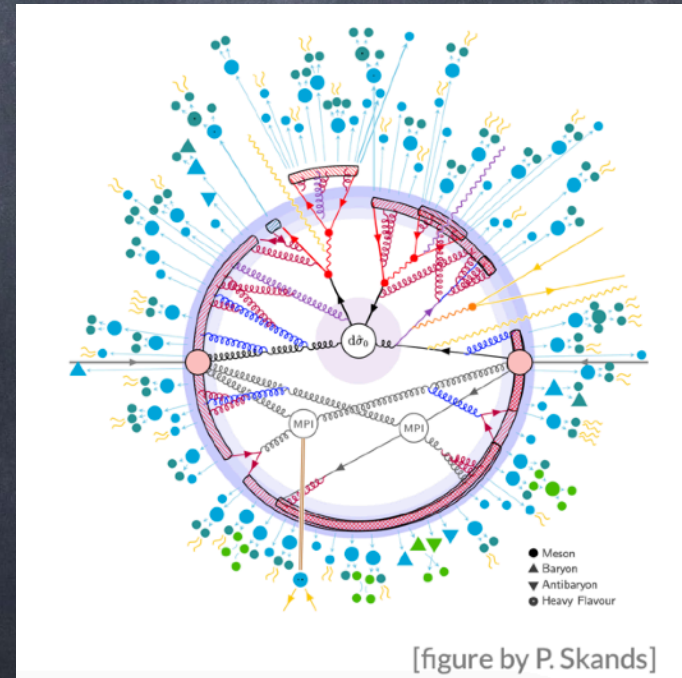
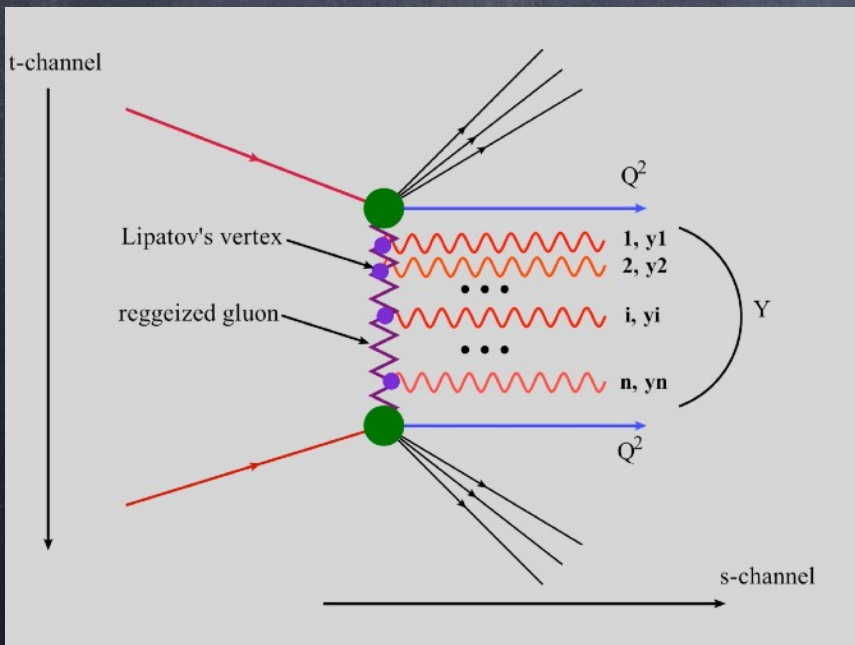
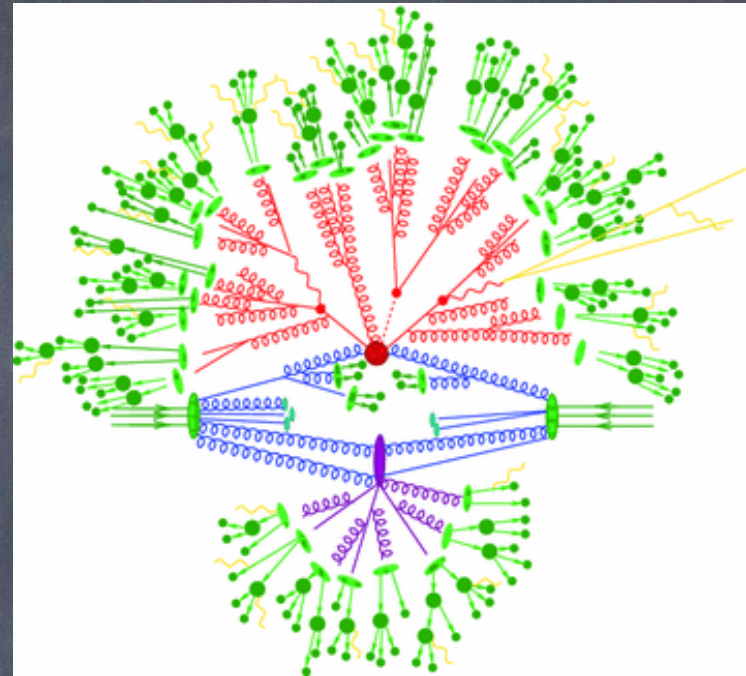
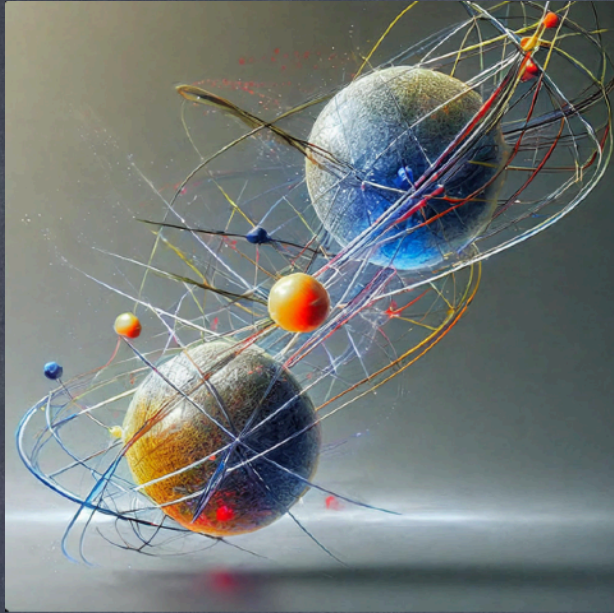
- C) They are irrelevant to practical calculations.

5. In the context of BFKL and saturation, what does the 'saturation scale' refer to?

- A) The minimum energy for saturation.

- B) The scale at which gluon recombination becomes significant, balancing density growth.

- C) A fixed momentum transfer value.

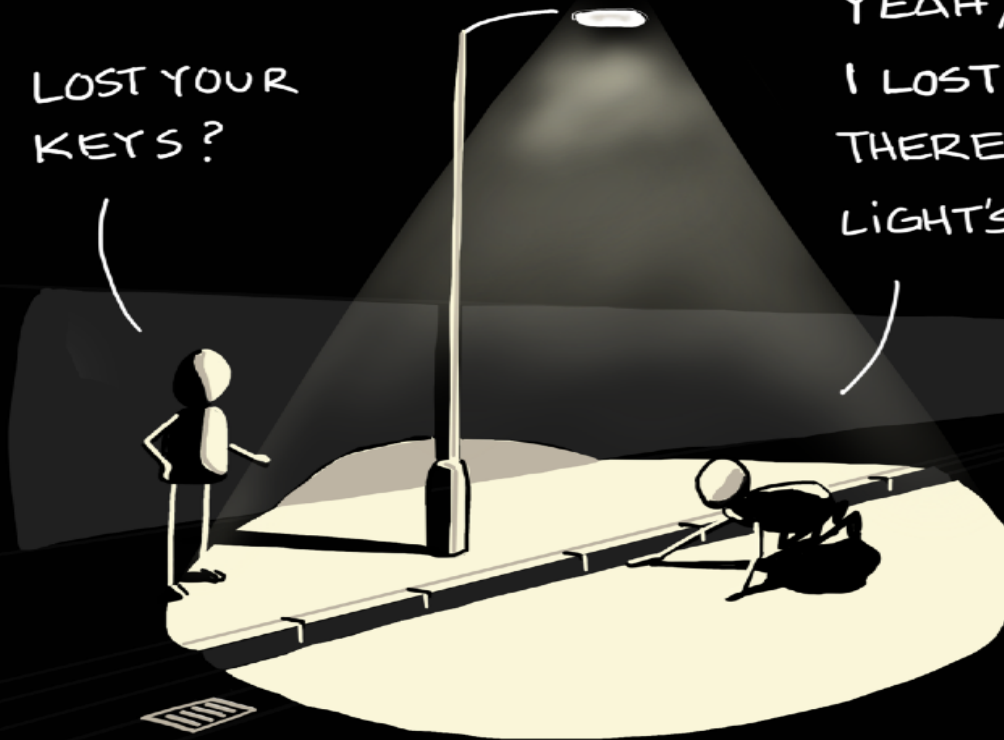


The streetlight effect

LOOKING UNDER THE LAMPPOST

LOST YOUR KEYS?

YEAH,
I LOST THEM OVER
THERE BUT THE
LIGHT'S BETTER HERE

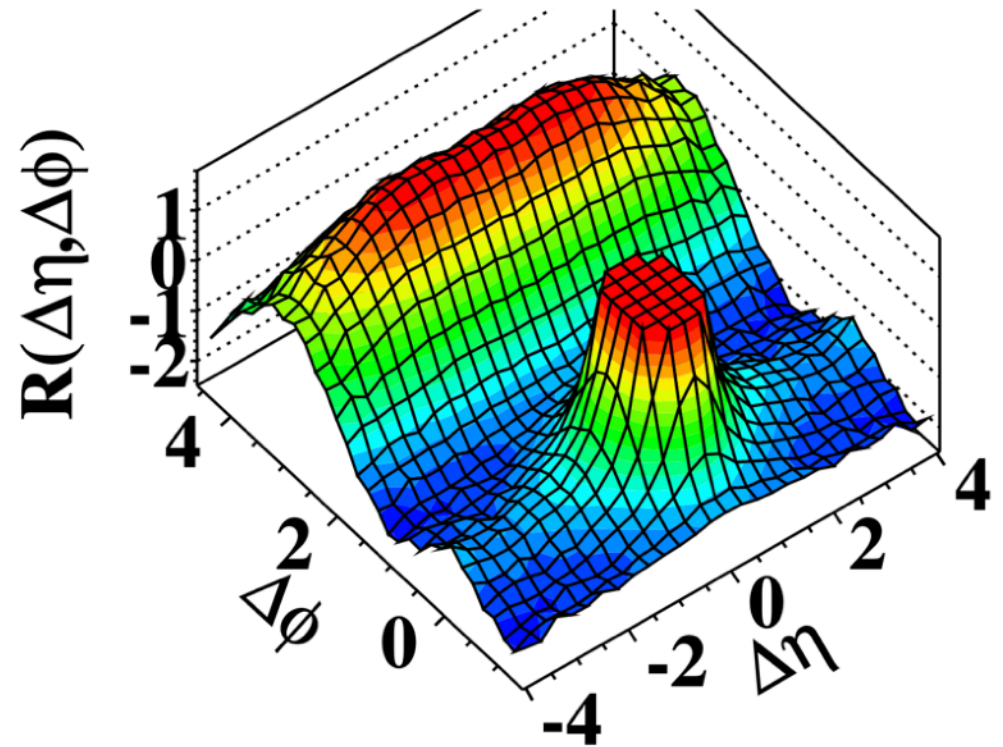


sketchplanations

The near-side ridge effect

- The study of the $\Delta\eta$ - $\Delta\phi$ correlation functions for proton-proton, proton-ion and ion-ion collisions, has drawn lots of attention in the last years. The correlation functions appear to have similar characteristics.
- Two “ridge-like structures”, the important here is the enhancement on the near side, relative azimuthal angle $\Delta\phi \approx 0$, that extends over a wide range in relative pseudorapidity ($|\Delta\eta| \approx$ up to 4).
- That long-range near-side correlation is known as the “ridge”.

(d) CMS $N \geq 110$, $1.0 \text{ GeV}/c < p_T < 3.0 \text{ GeV}/c$



Correlation functions

- The two-particle correlation function is often defined in pseudorapidity and azimuthal space as

$$C(\Delta\eta, \Delta\phi) = \frac{S(\Delta\eta, \Delta\phi)}{B(\Delta\eta, \Delta\phi)}$$

- S denotes the signal distribution which is built with particle pairs from the same event. B stands for the background distribution which involves particle pairs taken from different events; $\Delta\eta = \eta_1 - \eta_2$ and $\Delta\phi = \phi_1 - \phi_2$ are the pseudorapidity and azimuthal angle differences respectively between the particles with indices 1 and 2 which are labelling the trigger and associate particles.

- event1 = (1,2,3,4), event2 = (i,ii,iii,iv):

signal \rightarrow pairs {(1,2), (1,3), (1,4), (2,3), (2,4), (3,4)}

background \rightarrow pairs {(1,i), (1,ii), (1,iii), (1,iv), (2,i), (2,ii), (2,iii), ...}

Correlation functions

- The two-particle correlation function is often defined in pseudorapidity

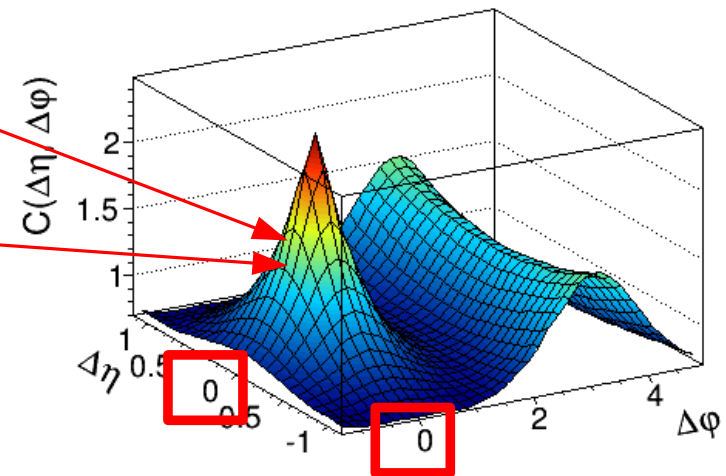
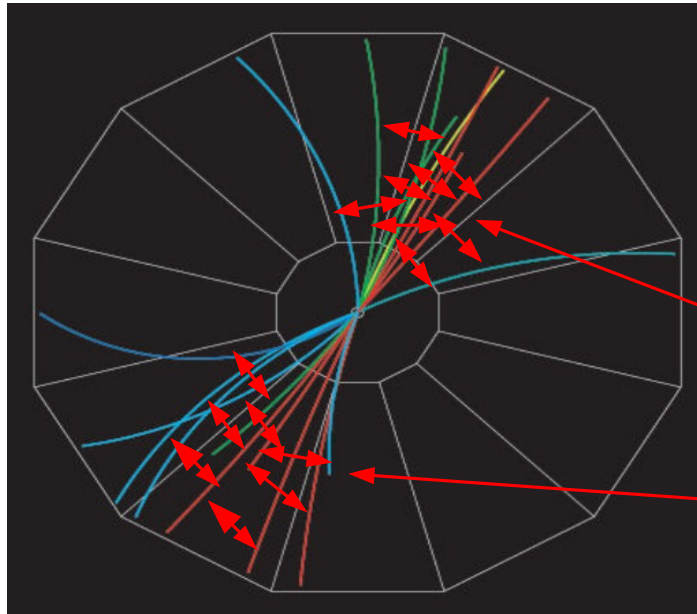
and azimuthal space as
$$C(\Delta\eta, \Delta\phi) = \frac{S(\Delta\eta, \Delta\phi)}{B(\Delta\eta, \Delta\phi)}$$

$$\tilde{\rho}(y, \vec{p}_T) = \frac{1}{\sigma_{\text{in}}} \frac{d^3\sigma}{d^3p} = \frac{1}{\sigma_{\text{in}}} \frac{d^3\sigma}{dy d^2p_T} = \frac{1}{2\sigma_{\text{in}}} \frac{d^3\sigma}{dy d\phi dp_T^2}$$

$$\tilde{\rho}_2(y_1, \vec{p}_{T1}, y_2, \vec{p}_{T2}) = \frac{1}{\sigma_{\text{in}}} \frac{d^6\sigma}{d^3p_1 d^3p_2} = \frac{1}{\sigma_{\text{in}}} \frac{d^6\sigma}{dy_1 d^2p_{T1} dy_2 d^2p_{T2}} = \frac{1}{4\sigma_{\text{in}}} \frac{d^6\sigma}{dy_1 d\phi_1 dp_{T1}^2 dy_2 d\phi_2 dp_{T2}^2}$$

$$C(1, 2) = \frac{\tilde{\rho}_2(1, 2)}{\tilde{\rho}(1)\tilde{\rho}(2)} \quad C(\Delta y, \Delta\phi) = \frac{s(\Delta y, \Delta\phi)}{b(\Delta y, \Delta\phi)}$$

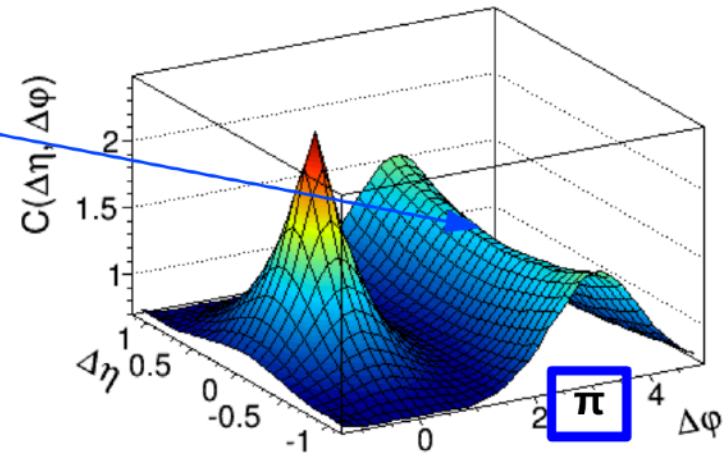
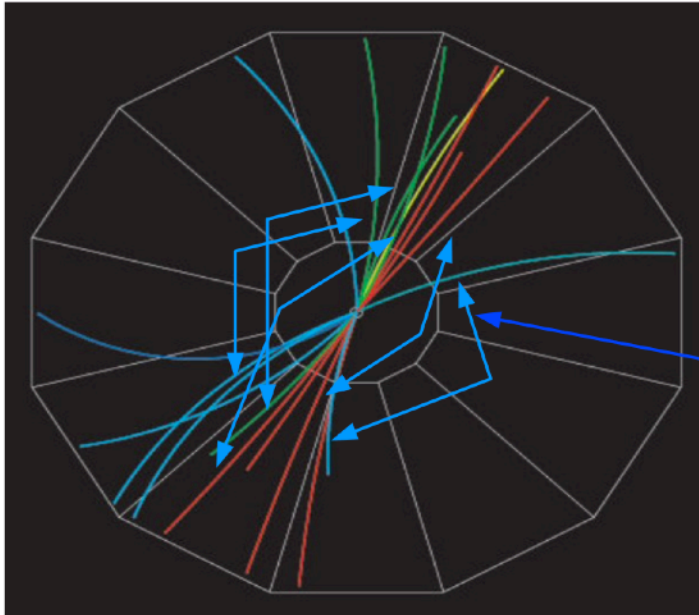
$\Delta\eta\Delta\phi$ two-particle angular correlations



For particles from the same jet (red):

- $\Delta\phi \sim 0$
- $\Delta\eta \sim 0$

$\Delta\eta\Delta\phi$ angular correlations



For particles from from back-to-back jets (blue):

- $\Delta\phi \sim \pi$
- $\Delta\eta \sim \text{const}$, if avaraged over many events

Angular correlations between the charged particles produced in pp collisions at ISR energies

K. Eggert, H. Frenzel, W. Thomé, B. Betev*, P. Darriulat, P. Dittmann, M. Holder,
 K.T. McDonald, T. Modis, H.G. Pugh**, K. Tittel, I. Derado, V. Eckardt, H.J. Gebauer,
 R. Meinke, O.R. Sander***, P. Seyboth

1975

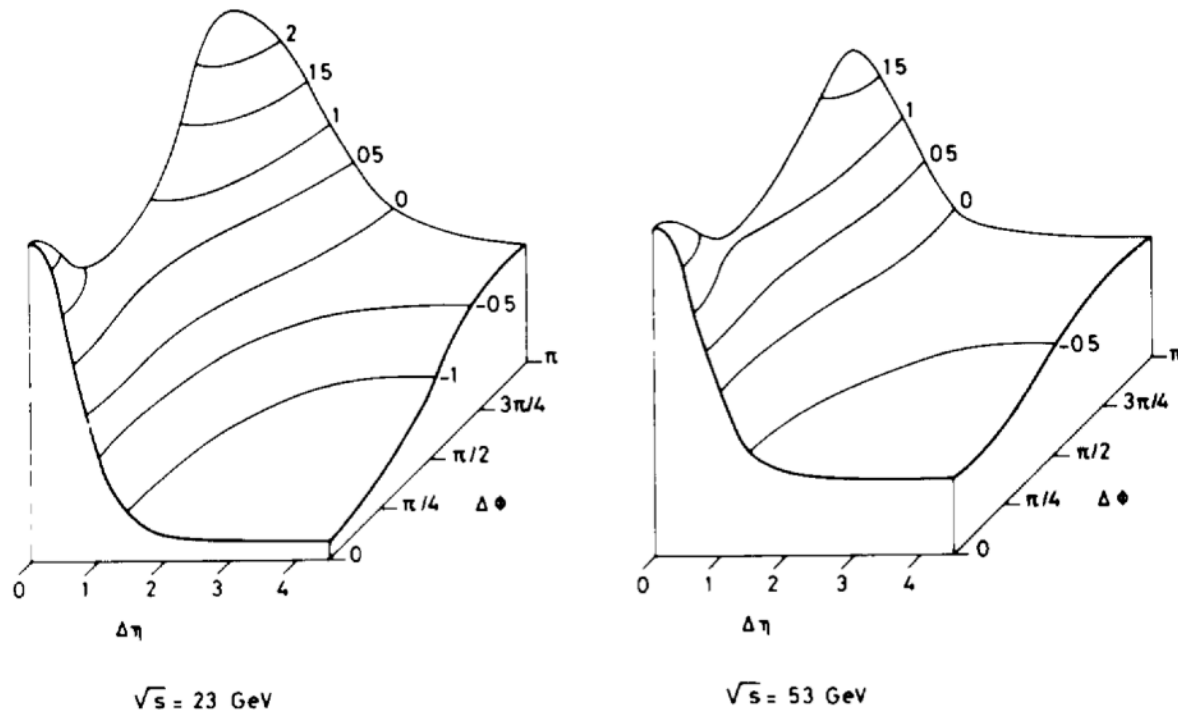


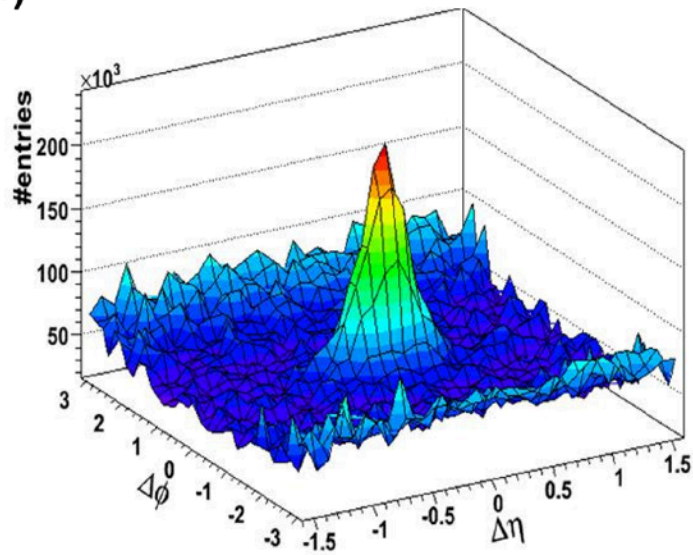
Fig 5 The measured angular correlation functions, $C^{\text{II}}(\Delta\eta, \Delta\phi)$, in units of 10^{-3} For clarity, smooth curves have been drawn through the data which have typical error bars of $\pm 0.4 \times 10^{-3}$

THE RIDGE EFFECT FROM p - p TO Pb-Pb
(AND BACK)*

HELENA BIAŁKOWSKA

on behalf of the CMS Collaboration

a)



b)

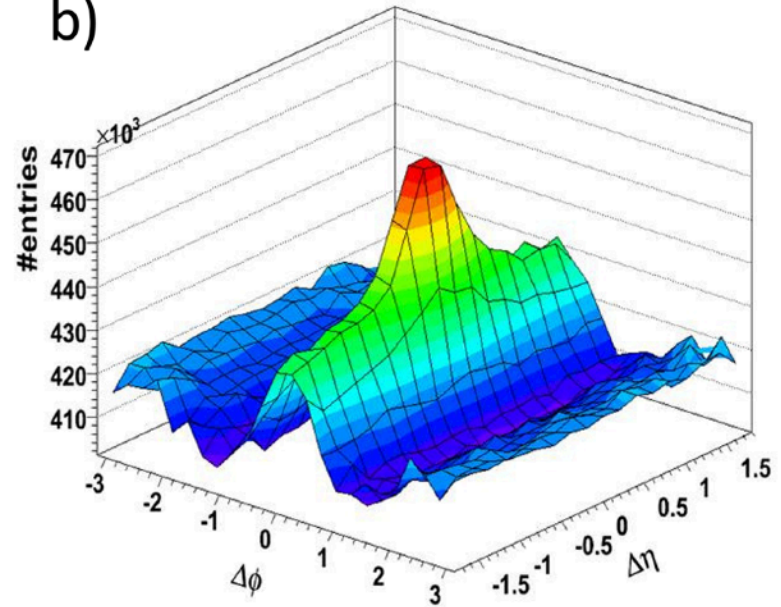


Fig. 1. Two particle correlation function for d -Au (left) and Au-Au (right) central events at $\sqrt{s_{NN}} = 200$ GeV from STAR experiment [2].

Measures of azimuthal anisotropy in high-energy collisions

Jean-Yves Ollitrault

Université Paris Saclay, CNRS, CEA, Institut de physique théorique, 91191 Gif-sur-Yvette, France

October 11, 2023

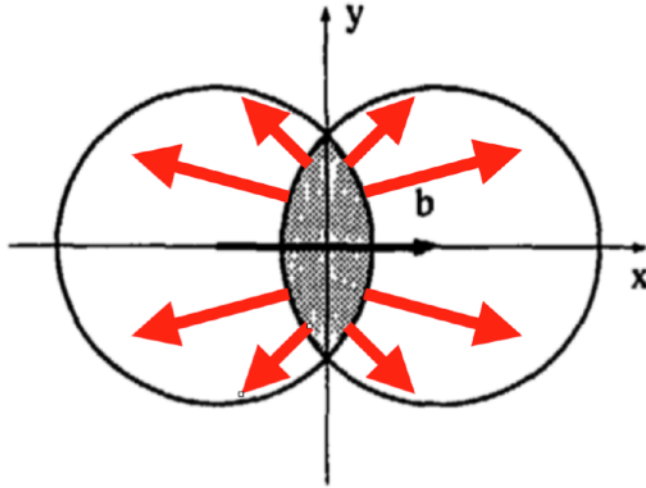


Fig. 3. Schematic view of a collision between two identical spherical nuclei at impact parameter b , in the transverse plane $z = 0$ [32]. Matter is produced in the shaded overlap area, where the participant nucleons lie. Red arrows represent pressure gradients within the produced matter. Outgoing particles typically go in the same directions as pressure gradients. This results in an elliptic anisotropy of their distribution.

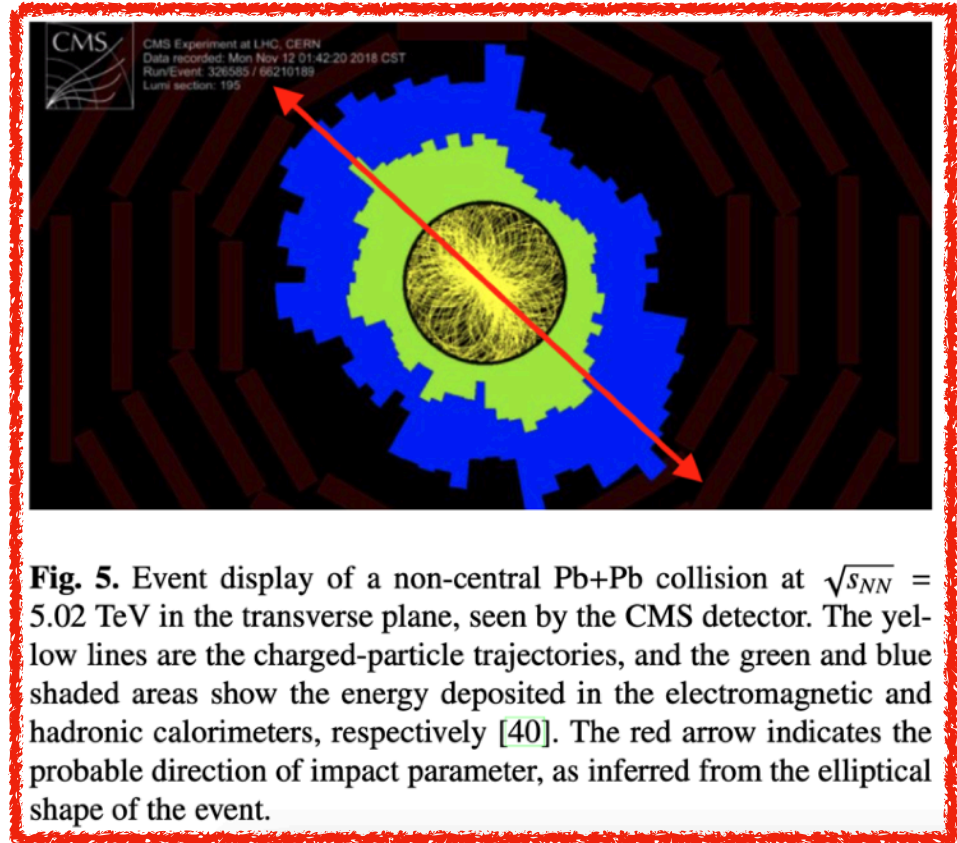
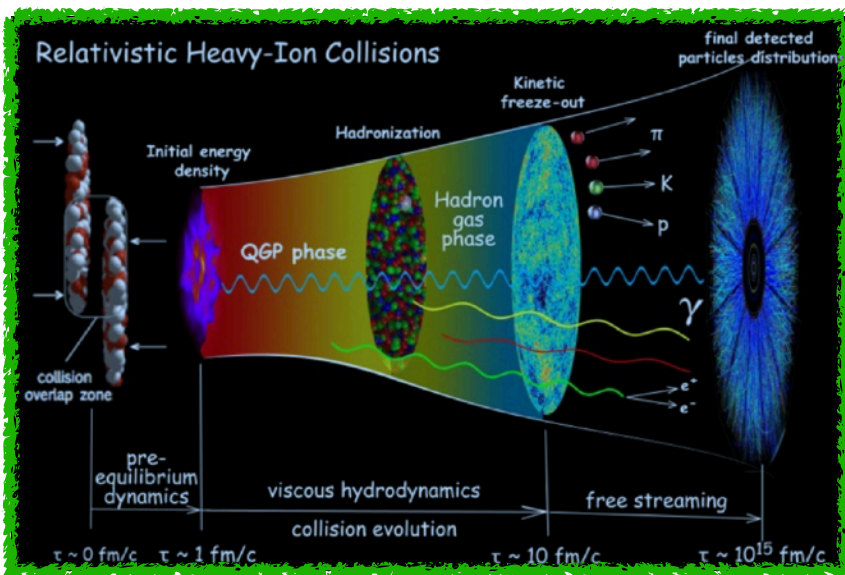


Fig. 5. Event display of a non-central Pb+Pb collision at $\sqrt{s_{NN}} = 5.02$ TeV in the transverse plane, seen by the CMS detector. The yellow lines are the charged-particle trajectories, and the green and blue shaded areas show the energy deposited in the electromagnetic and hadronic calorimeters, respectively [40]. The red arrow indicates the probable direction of impact parameter, as inferred from the elliptical shape of the event.

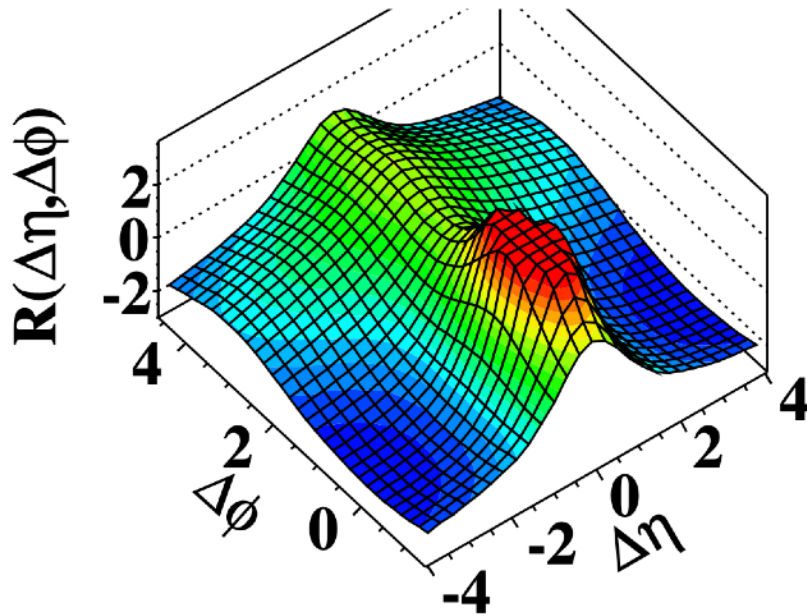


arXiv:1311.2574

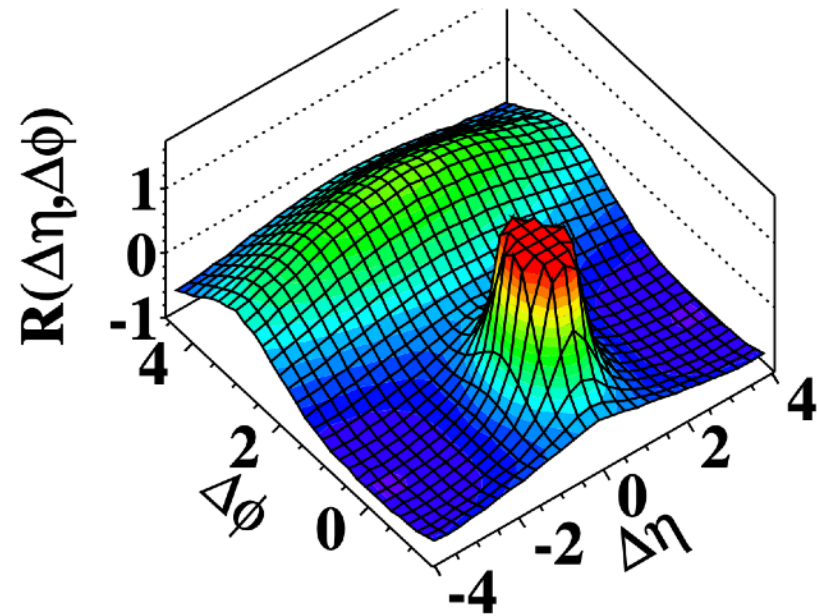
Observation of Long-Range, Near-Side Angular Correlations in Proton-Proton Collisions at the LHC

The CMS Collaboration*

(a) CMS MinBias, $p_T > 0.1 \text{ GeV}/c$



(b) CMS MinBias, $1.0 \text{ GeV}/c < p_T < 3.0 \text{ GeV}/c$

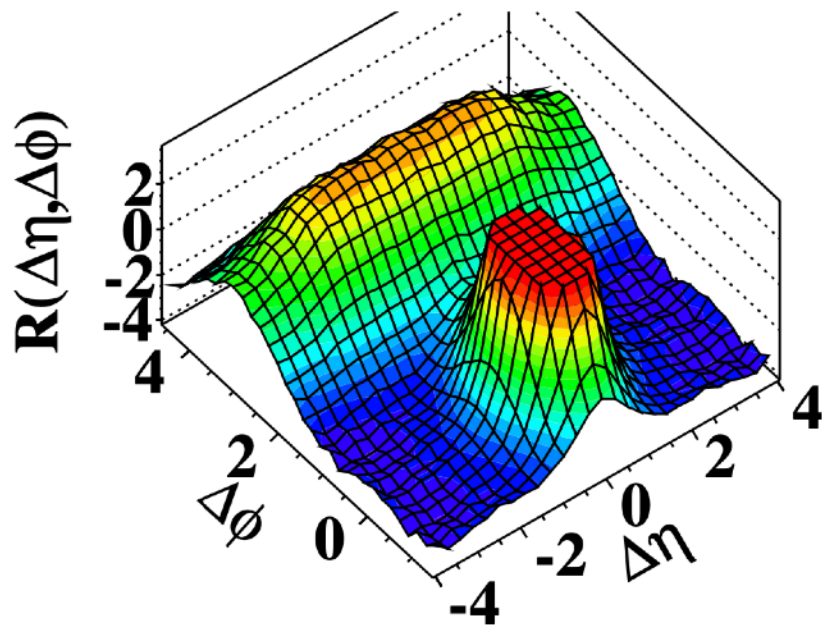


taken from

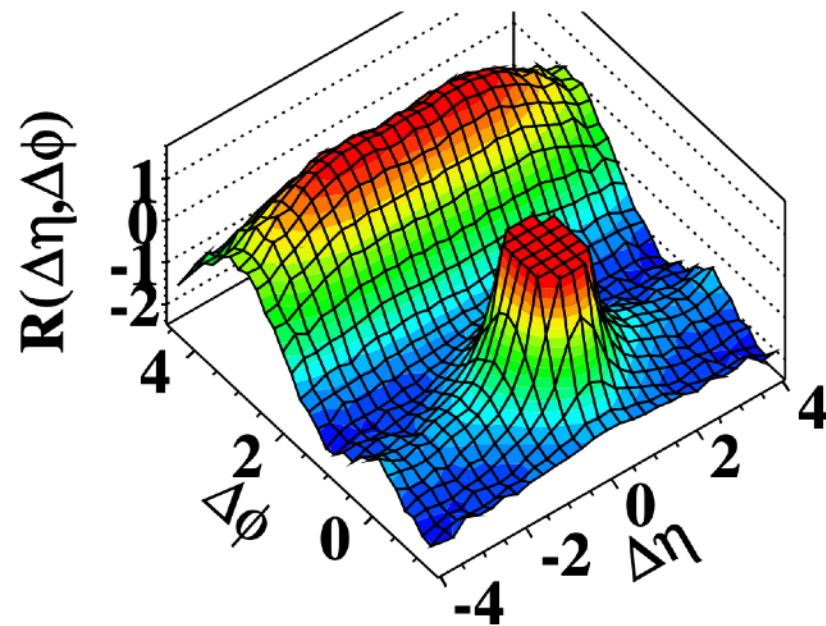
Observation of Long-Range, Near-Side Angular Correlations in Proton-Proton Collisions at the LHC

The CMS Collaboration*

(c) CMS $N \geq 110$, $p_T > 0.1 \text{ GeV}/c$



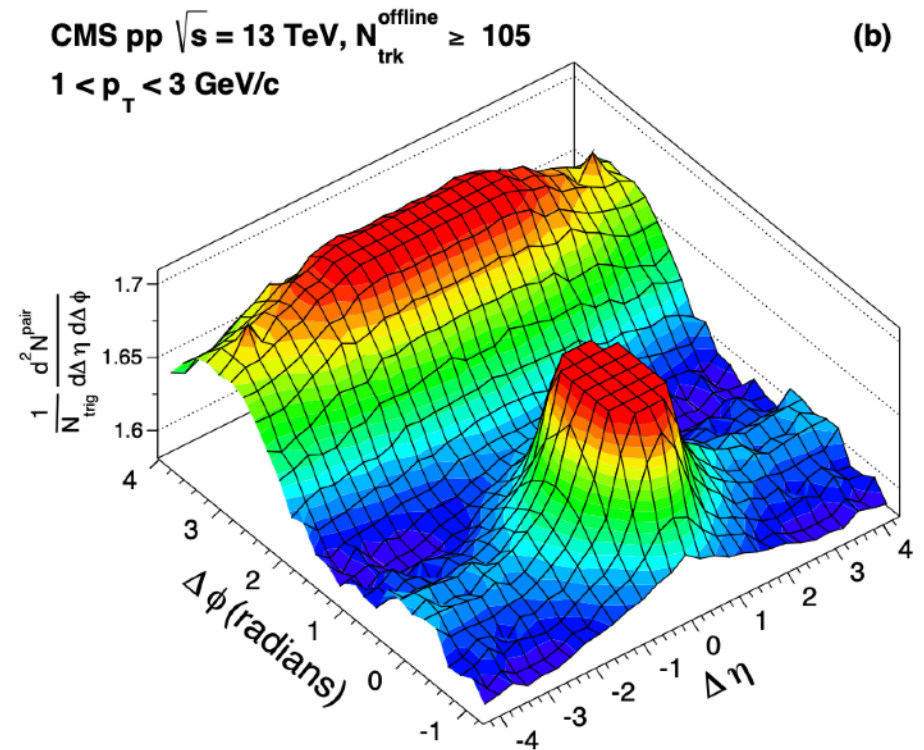
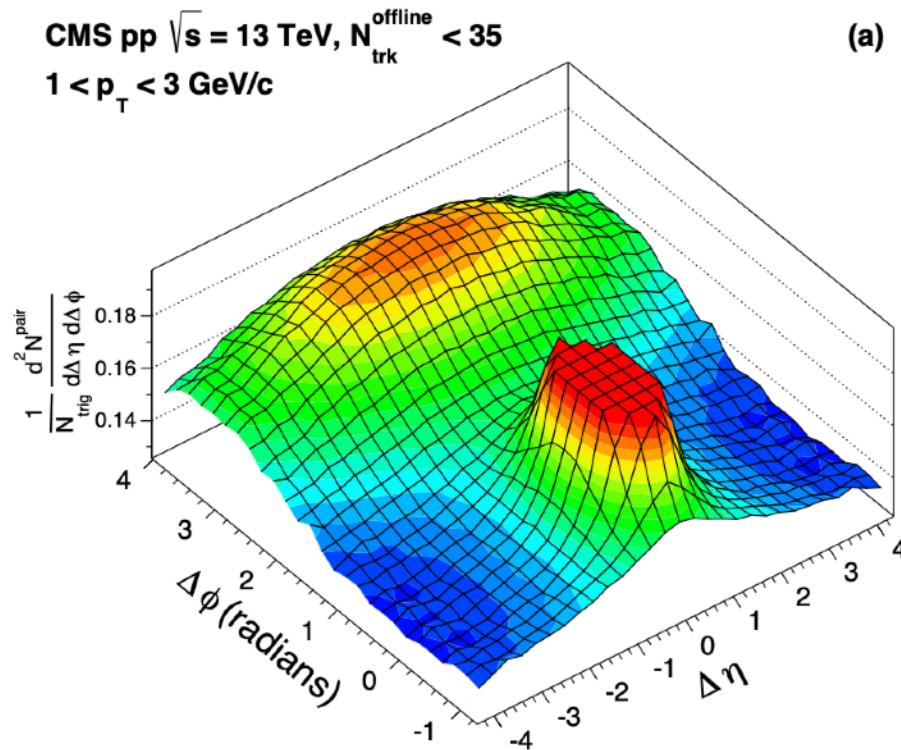
(d) CMS $N \geq 110$, $1.0 \text{ GeV}/c < p_T < 3.0 \text{ GeV}/c$



taken from

Measurement of long-range near-side two-particle angular correlations in pp collisions at $\sqrt{s} = 13$ TeV

The CMS Collaboration*

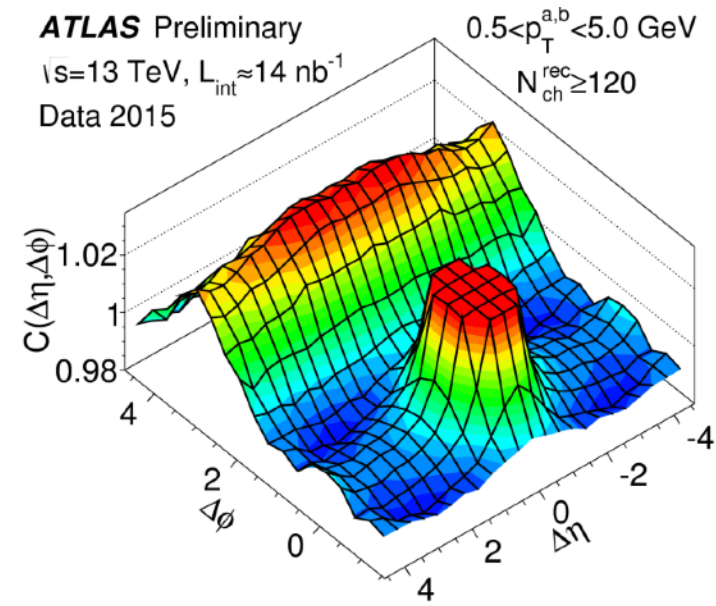
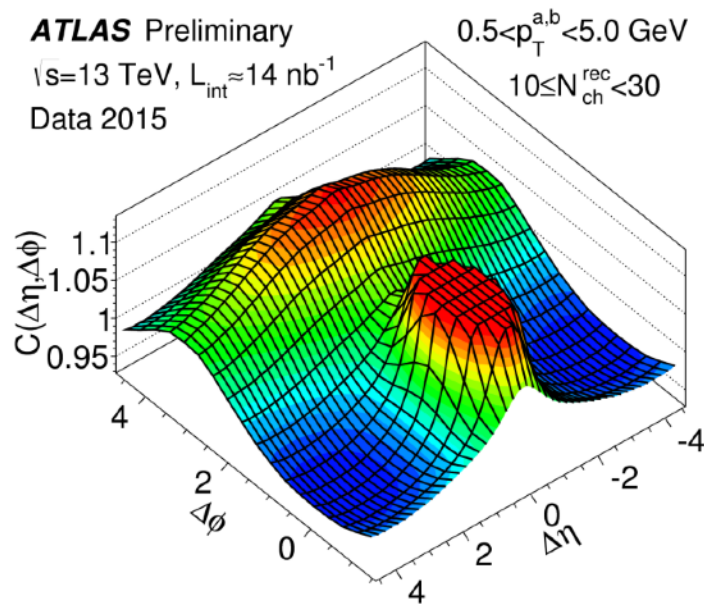


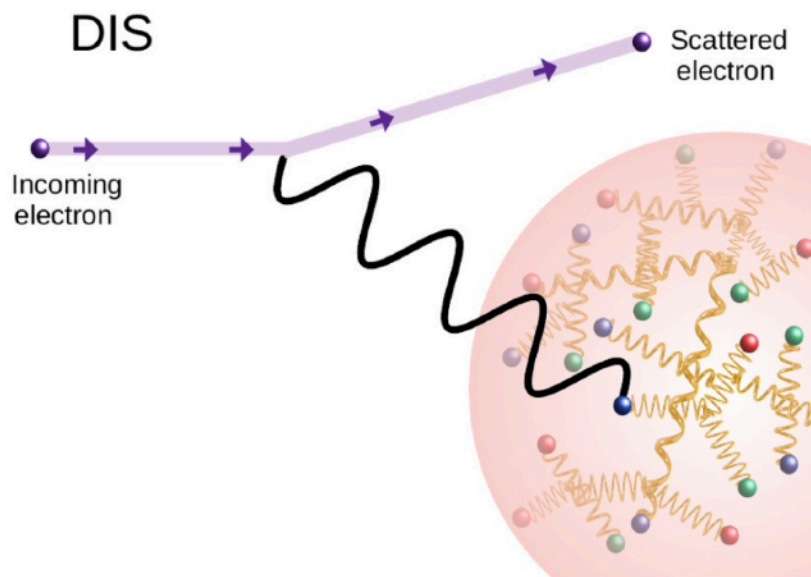
taken from <https://arxiv.org/pdf/1510.03068.pdf>

ATLAS measurements of the ridge in proton-proton collisions at 13 TeV

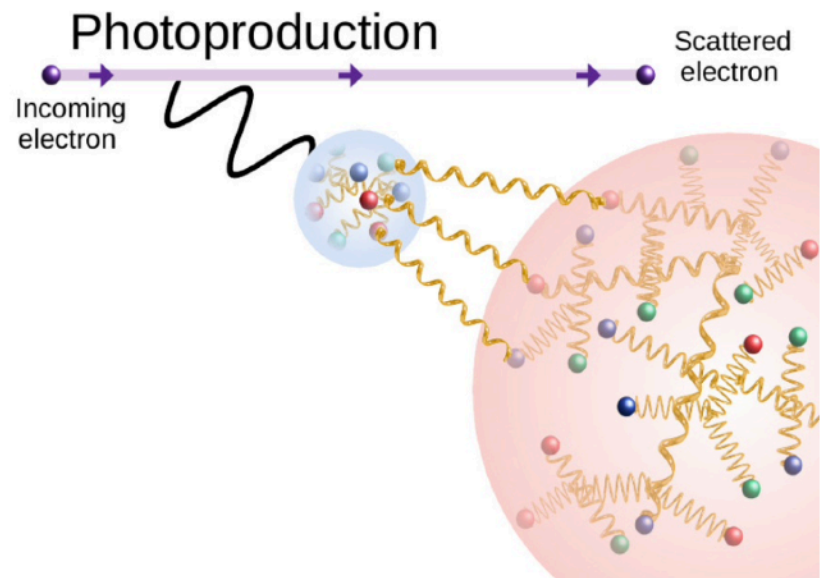
ATLAS has completed a preliminary measurement of two-particle correlations in 13 TeV proton-proton collisions at the LHC using data collected during a low-luminosity run in June 2015

24 July 2015 | By [ATLAS Collaboration](#)





(a) Neutral current deep inelastic scattering.



(b) Resolved photoproduction.

Azimuthal correlations in photoproduction and deep inelastic ep scattering at HERA

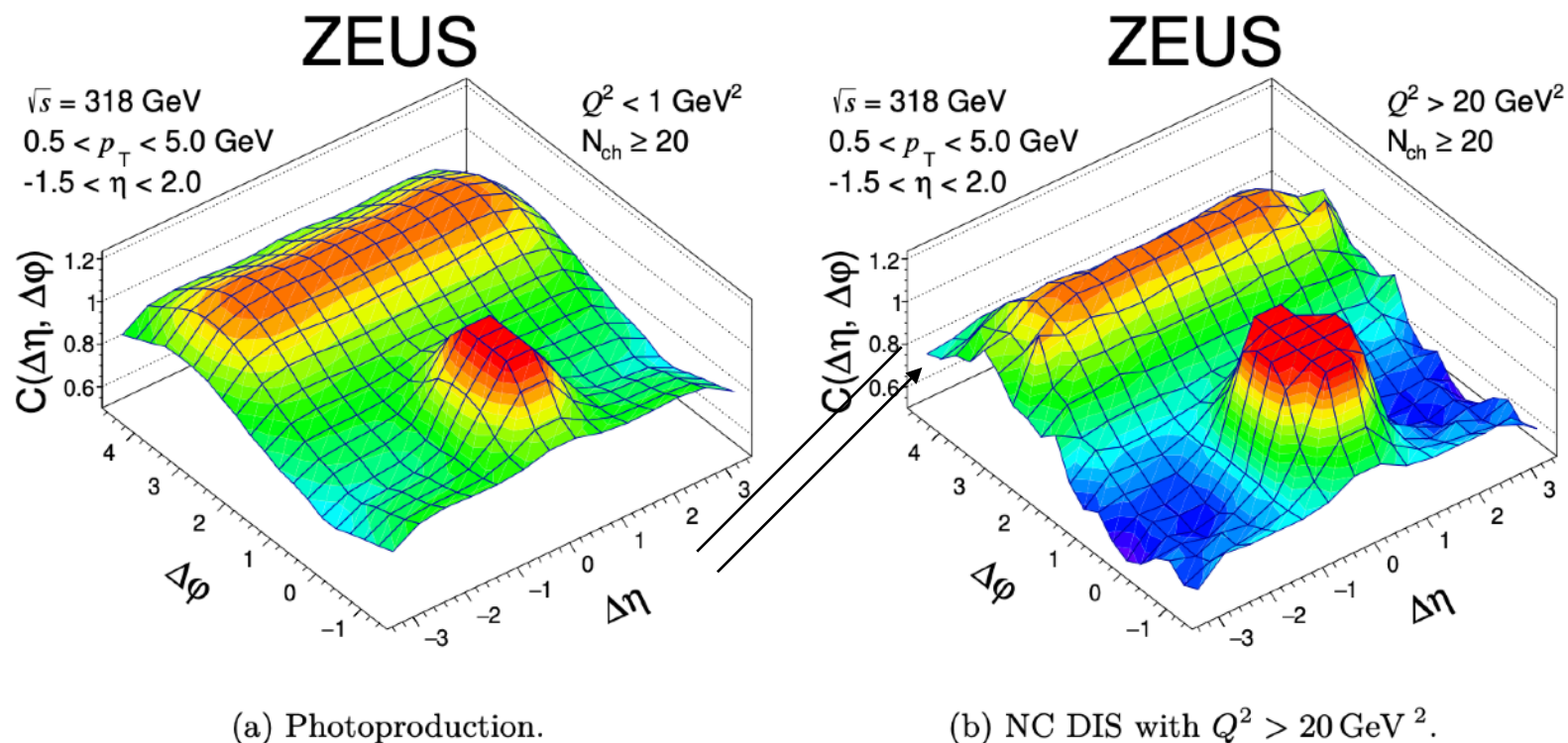


Figure 3. Two-particle correlation $C(\Delta\eta, \Delta\phi)$ in (a) photoproduction and (b) NC DIS with $Q^2 > 20 \text{ GeV}^2$. The peak near the origin has been truncated for better visibility of the finer structures of the correlation. The plot has been symmetrised along $\Delta\eta$. No statistical or systematic uncertainties are shown.

is no indication of a double ridge, which was observed in high-multiplicity $p + p$ and $p + \text{Pb}$

Measurements of Two-Particle Correlations in e^+e^- Collisions at 91 GeV with ALEPH Archived Data

Anthony Badea,¹ Austin Baty,¹ Paoti Chang,² Gian Michele Innocenti,¹ Marcello Maggi,³
Christopher McGinn,¹ Michael Peters,¹ Tzu-An Sheng,² Jesse Thaler,¹ and Yen-Jie Lee^{1,*}

¹*Massachusetts Institute of Technology, Cambridge, Massachusetts, USA*

²*National Taiwan University, Taipei, Taiwan*

³*INFN Sezione di Bari, Bari, Italy*

(Dated: November 27, 2019)

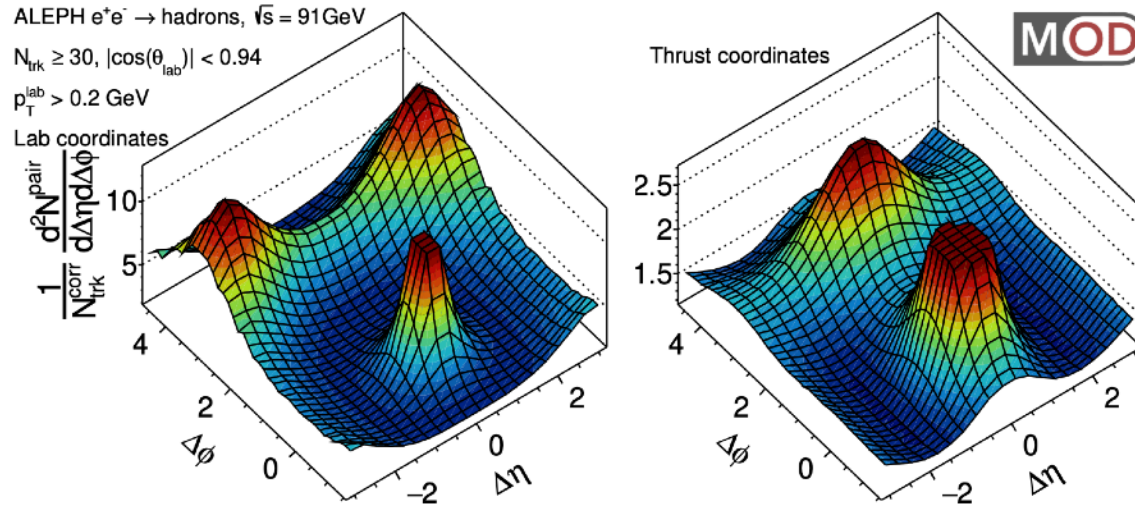


FIG. 1: Two-particle correlation functions for events with the number of charged particle tracks in the event $N_{\text{trk}} \geq 30$ in the lab coordinates (left) and thrust coordinates (right) analyses. The sharp near-side peaks arise from jet correlations and have been truncated to better illustrate the structure outside that region.

“In contrast to the results from high multiplicity pp, pA and AA collisions, where long-range correlations with large pseudorapidity gap are observed, no significant enhancement of long-range correlations is observed in e^+e^- collisions. The data are compared to generators that do not include additional final-state interactions of the outgoing partons. The results are better described by the pythia and sherpa generators than herwig.”

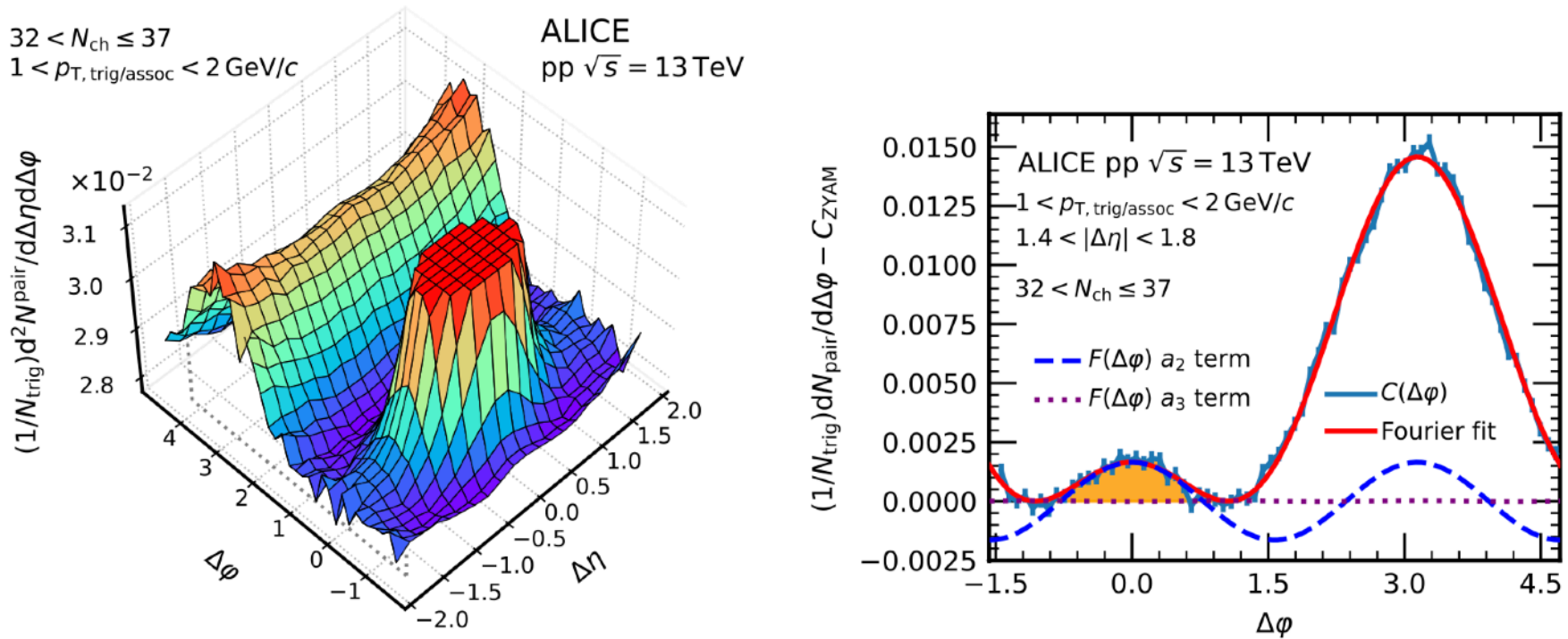
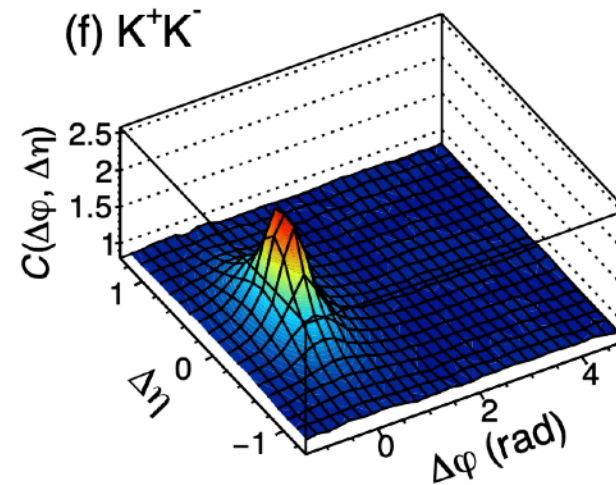
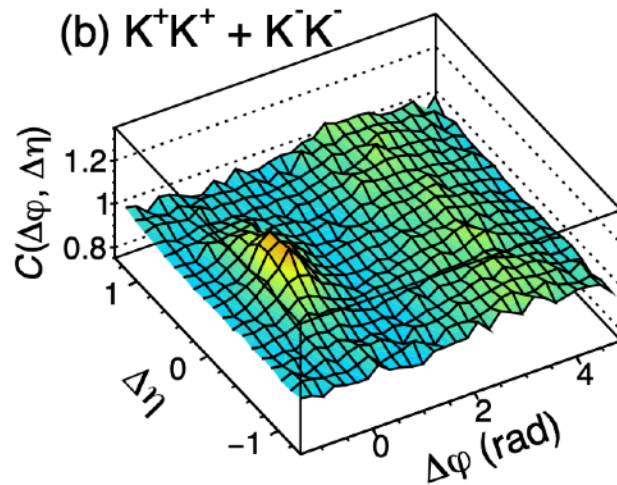
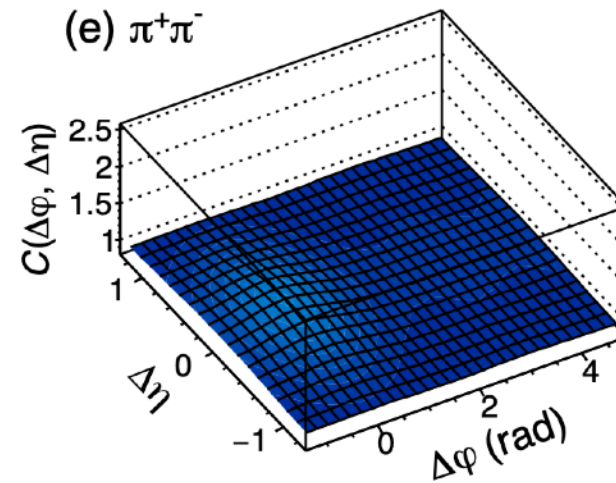
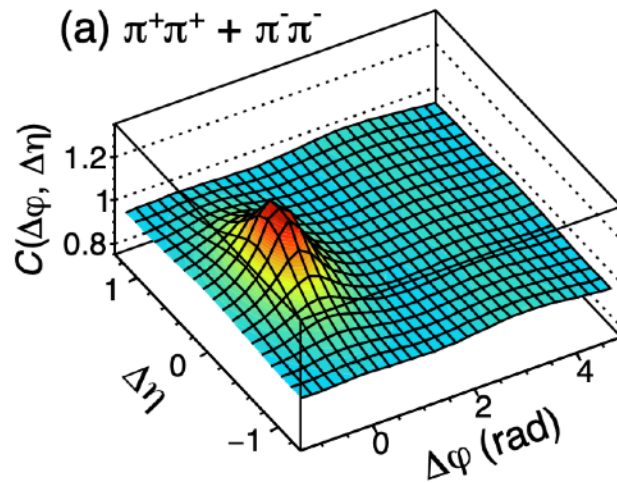


Figure 1: Two-particle per-trigger yield measured for charged track pairs with $1 < p_{\text{T, trig}} < 2 \text{ GeV}/c$ and $1 < p_{\text{T, assoc}} < 2 \text{ GeV}/c$ within the multiplicity range $32 < N_{\text{ch}} \leq 37$. The jet fragmentation peak has been truncated to ensure a better visibility of the long-range structure. The right panel shows the zero-suppressed projection to $\Delta\phi$ overlaid with $F(\Delta\phi)$ (red line) and the area in which the ridge yield is extracted (shaded area). The blue and purple lines represent the second and third harmonic terms of $F(\Delta\phi)$.

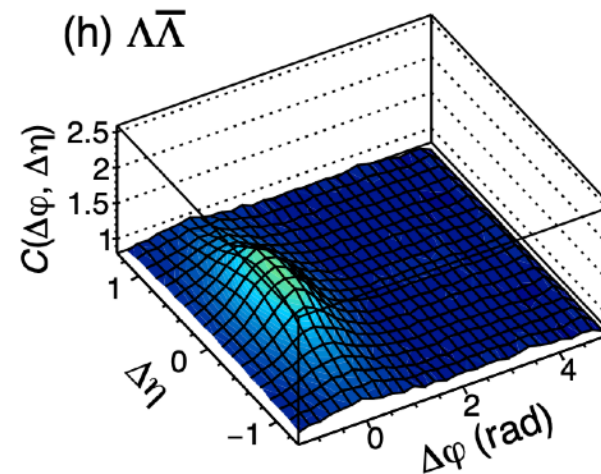
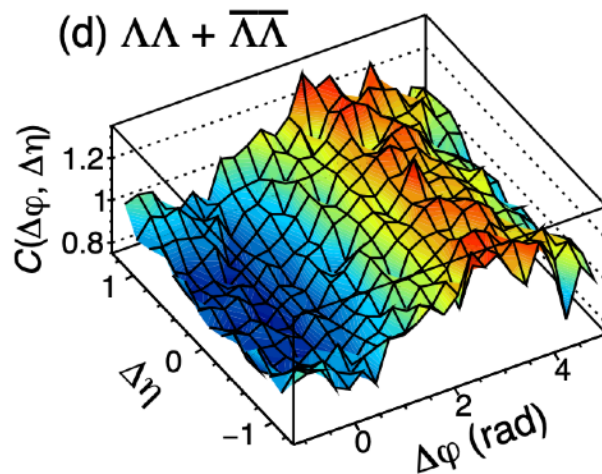
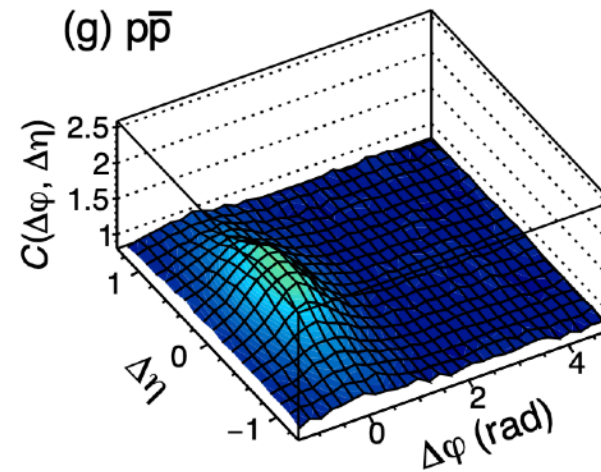
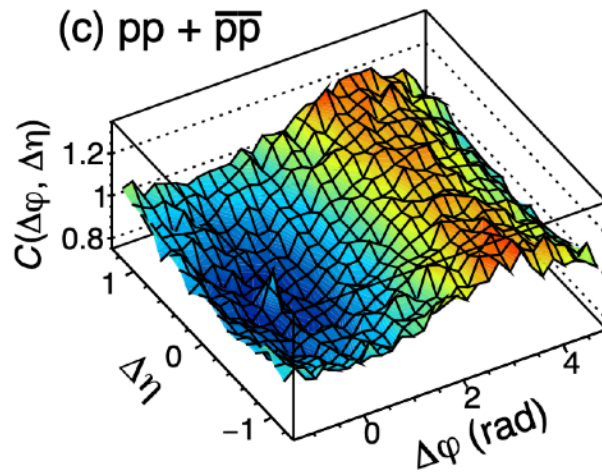
Insight into particle production mechanisms via angular correlations of identified particles in pp collisions at $\sqrt{s} = 7$ TeV

ALICE Collaboration*



Insight into particle production mechanisms via angular correlations of identified particles in pp collisions at $\sqrt{s} = 7$ TeV

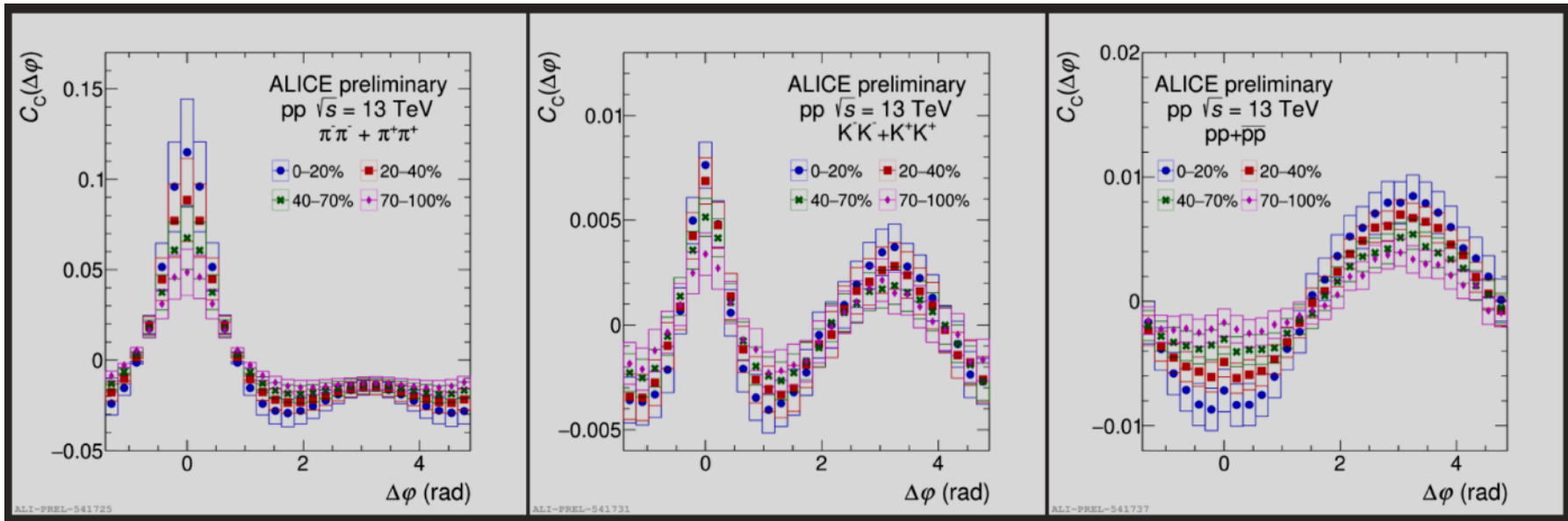
ALICE Collaboration*



1

Two-particle angular correlations of identified particles in pp collisions at $\sqrt{s} = 13$ TeV with ALICE

Daniela Ruggiano (for the ALICE Collaboration)



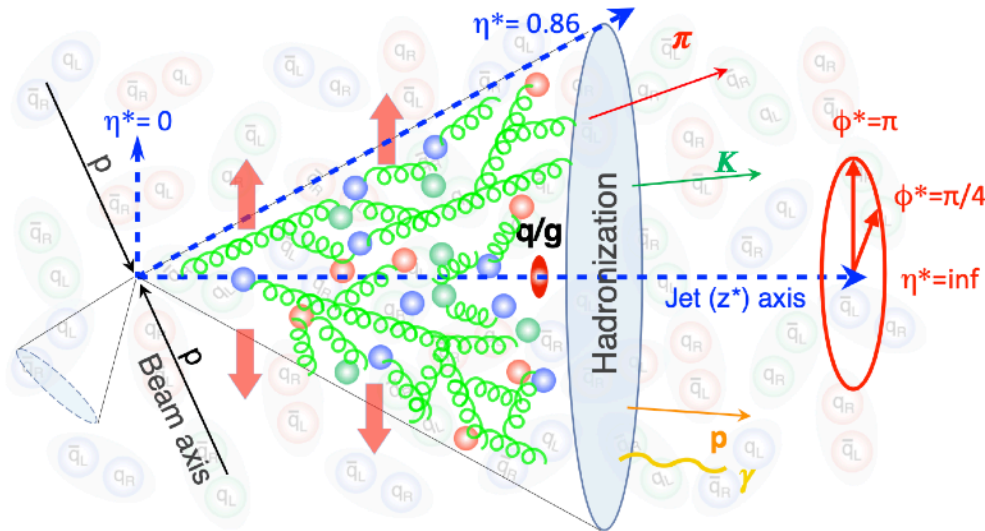
“In particular, the baryon–baryon (antibaryon–antibaryon) pairs show a considerable depletion called anticorrelation”

Observation of enhanced long-range elliptic anisotropies inside high-multiplicity jets in pp collisions at $\sqrt{s} = 13$ TeV

CMS Collaboration

28 December 2023

Submitted to Phys. Rev. Lett.



CMS

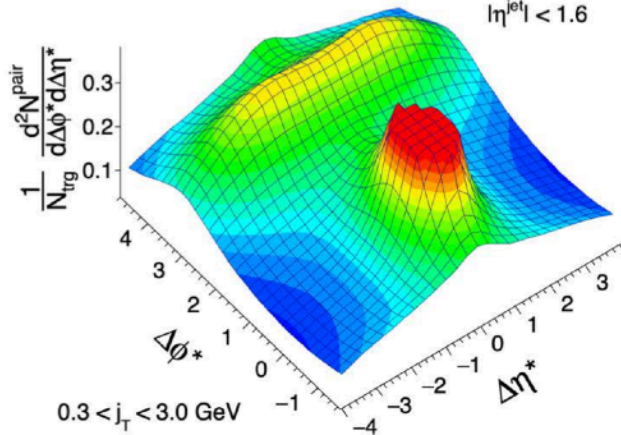
$\langle N_{ch}^j \rangle = 26$

138 fb⁻¹ (pp 13 TeV)

Anti $k_{T,R}=0.8$

$p_T^{\text{jet}} > 550$

$|\eta^{\text{jet}}| < 1.6$



CMS

$\langle N_{ch}^j \rangle = 101$

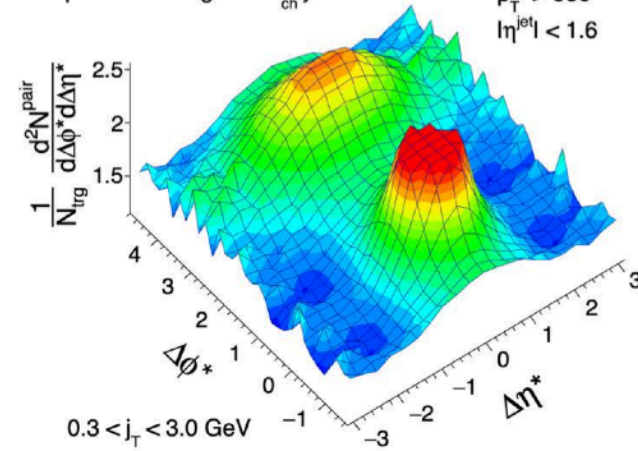
Top 0.0023% highest- N_{ch}^j jets

138 fb⁻¹ (pp 13 TeV)

Anti $k_{T,R}=0.8$

$p_T^{\text{jet}} > 550$

$|\eta^{\text{jet}}| < 1.6$



The near-side ridge effect

- There are two mainstream mechanisms (and many others) that give an explanation of the ridge effect in small systems (proton-proton and proton-ion collisions)
- The "domain structure of the target" and the "glasma graph approach" —**initial state mechanism**— within the Color Glass Condensate effective field theory (CGC).
- The viscous relativistic hydrodynamics —**final state mechanism**— strong final state evolution described by hydrodynamics. Collectivity that implies a strongly coupled quark gluon plasma (QGP) that flows.

The near-side ridge effect

- The study of two-particle correlations is a powerful tool in exploring the underlying mechanisms of particle production.
- How do ridge-like structures emerge in perturbative Quantum Chromodynamics (QCD) in multiparticle production?
- Up to which degree can the ridge effect in proton-proton collisions be explained by the first principles of QCD and how does it generalize to heavy ion collisions?

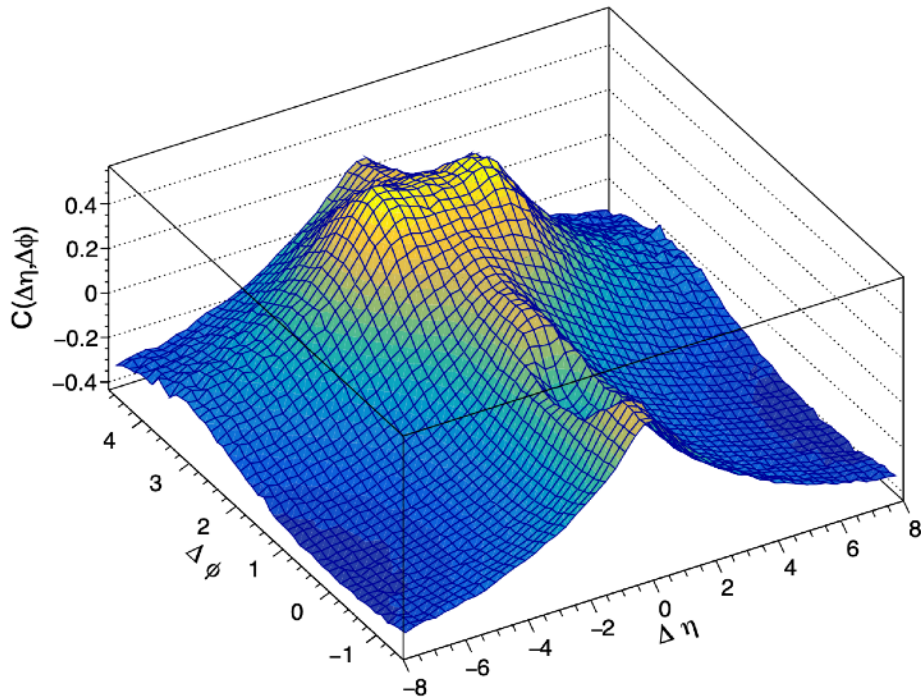
**one step between: from
particles to minijets
(partons)**

First principles pQCD?

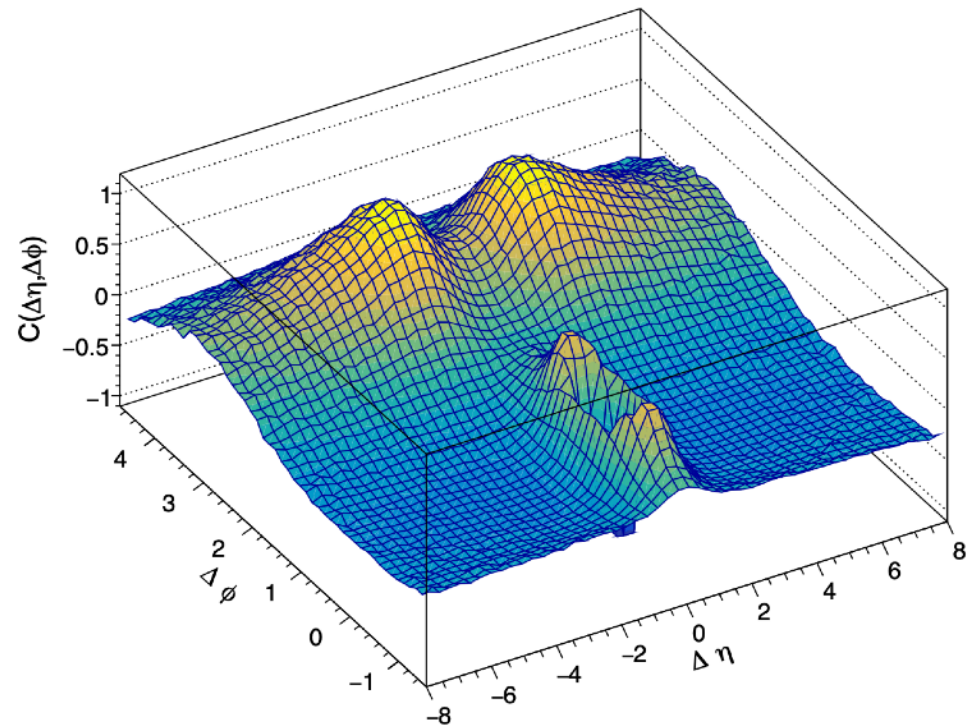
- The study of particle-particle angular correlations is an essential tool to probe the relevant dynamics that governs the strong force.
- The interpretation of the ridge in proton-proton collisions is a huge challenge but at the same time an opportunity to probe QCD in unique ways.
- Various attempts so far to give a full account of the cause behind the ridge have not succeeded.
- It could be that novel phenomena or even new physics are behind the correct interpretation of the long-range correlations, however, this possibility cannot be seriously explored before we fully understand the role of QCD. In particular, the role of perturbative QCD. First principles QCD, that is, avoiding any modelling to the extent that such an effort is feasible, needs to be confronted with the ridge effect on the basis of Monte Carlo simulations against the correlation distributions that are available from the experimental data.

Pythia simulations – pp

partonic min pT = 1 GeV
minijet min pT = 1 GeV, R = 0.5



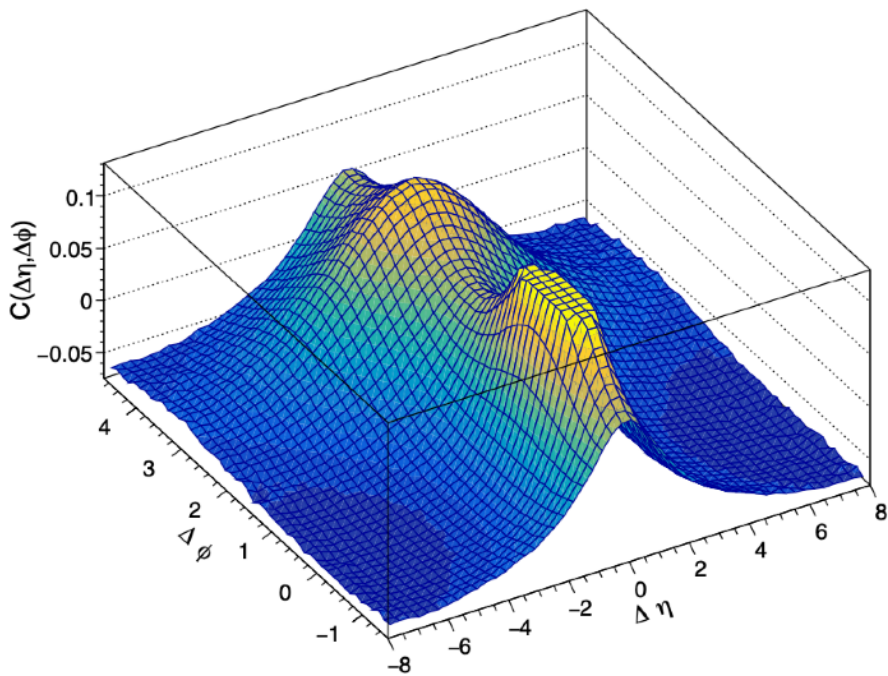
Partons



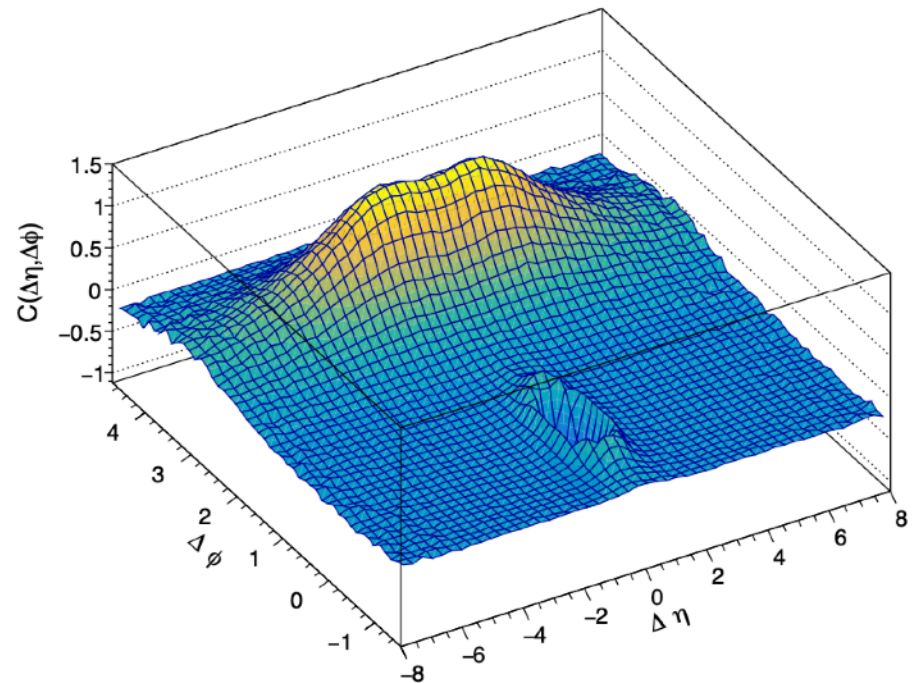
Minijets

Pythia simulations – pp

partonic min pT = 5 GeV
minijet min pT = 5 GeV, R = 0.5



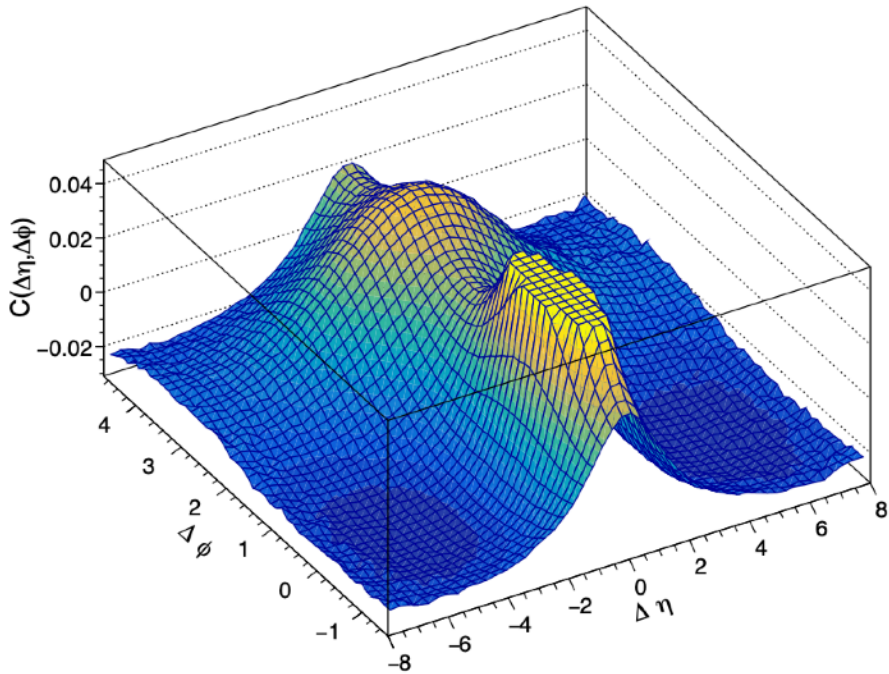
Partons



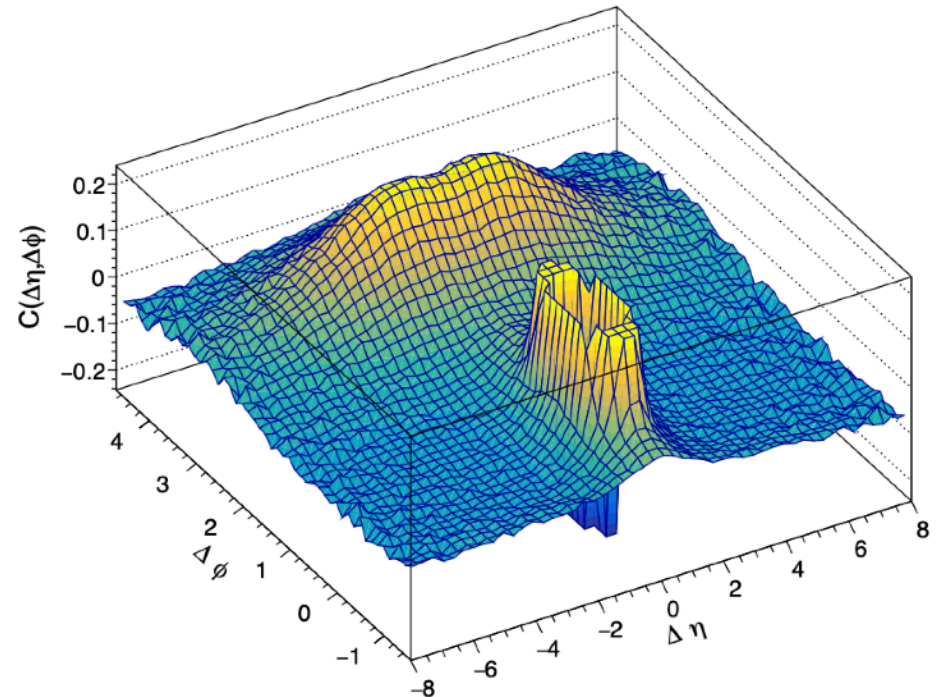
Minijets

Pythia simulations – pp

partonic min pT = 20 GeV
of minijets > 10
minijet min pT = 5 GeV, R = 0.5



Partons



Minijets

Pythia simulations – pp

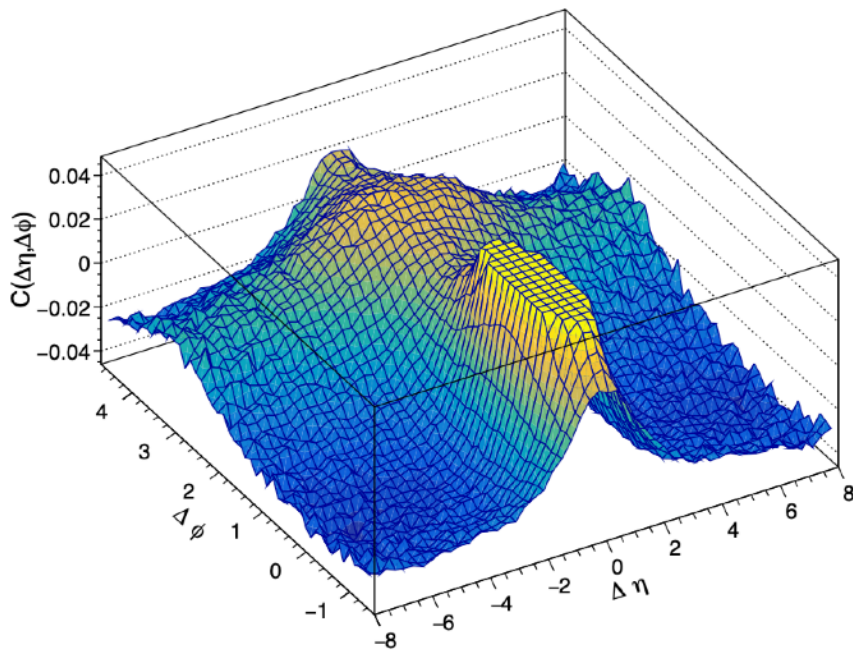
partonic min pT = 20 GeV

of minijets > 10

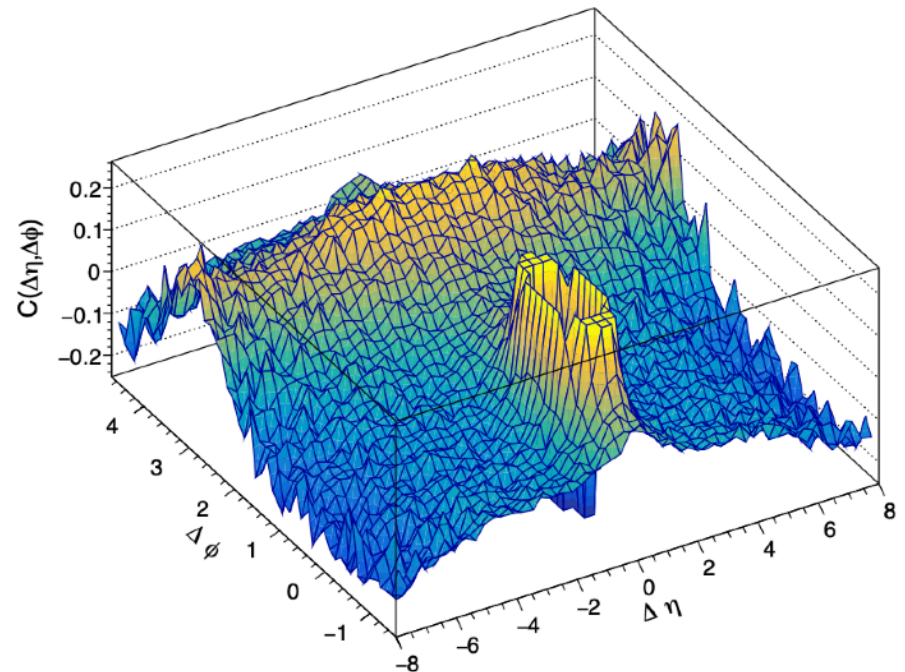
minijet min pT = 5 GeV, R = 0.5

$1 < \text{ptForward}/\text{ptBackward} < 1.5$ (and reverse)

$4 < \max \Delta Y < 9.4$



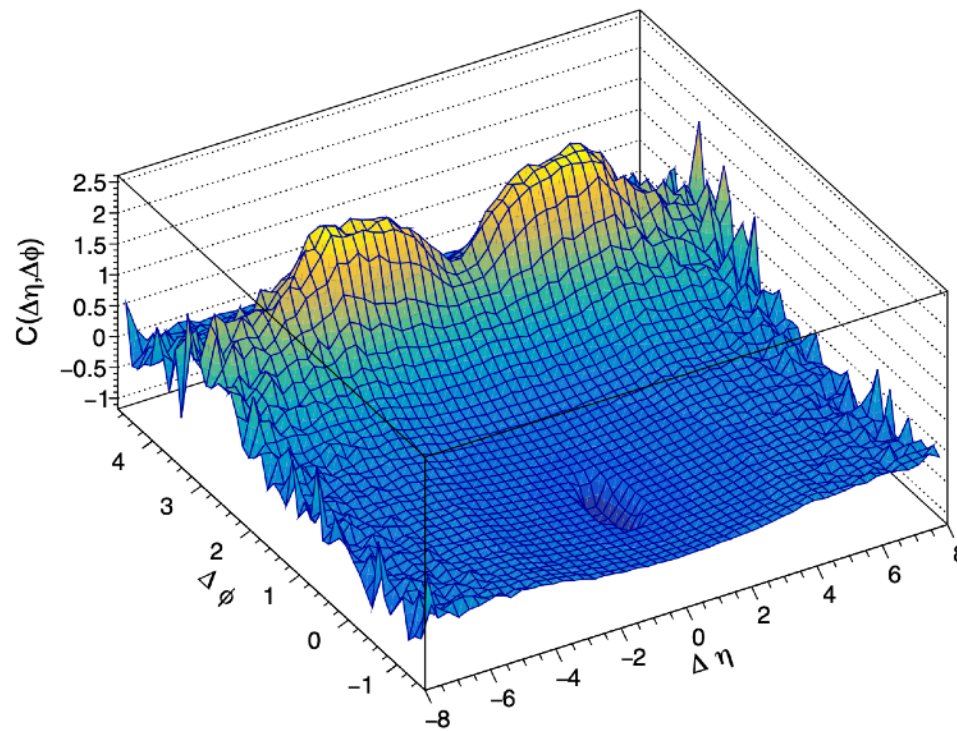
Partons



Minijets

BFKLex simulations — pp

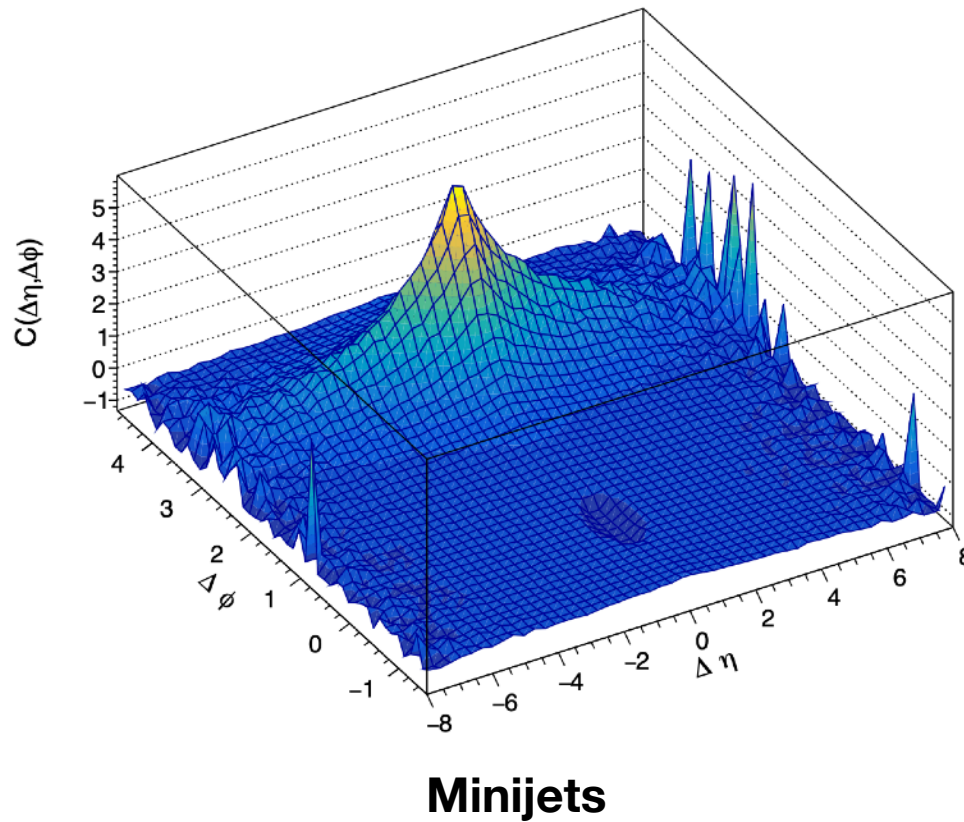
partonic min pT = 5 GeV
minijet min pT = 5 GeV, R = 0.5



Minijets

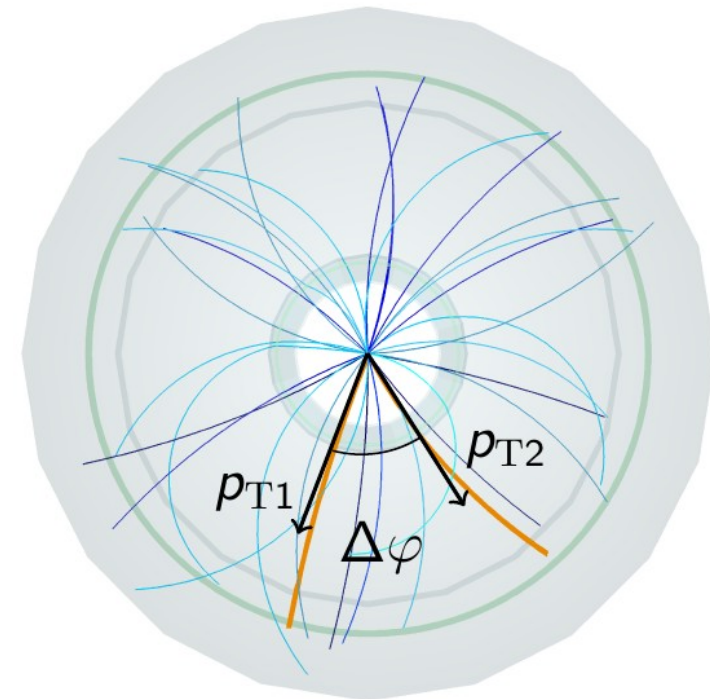
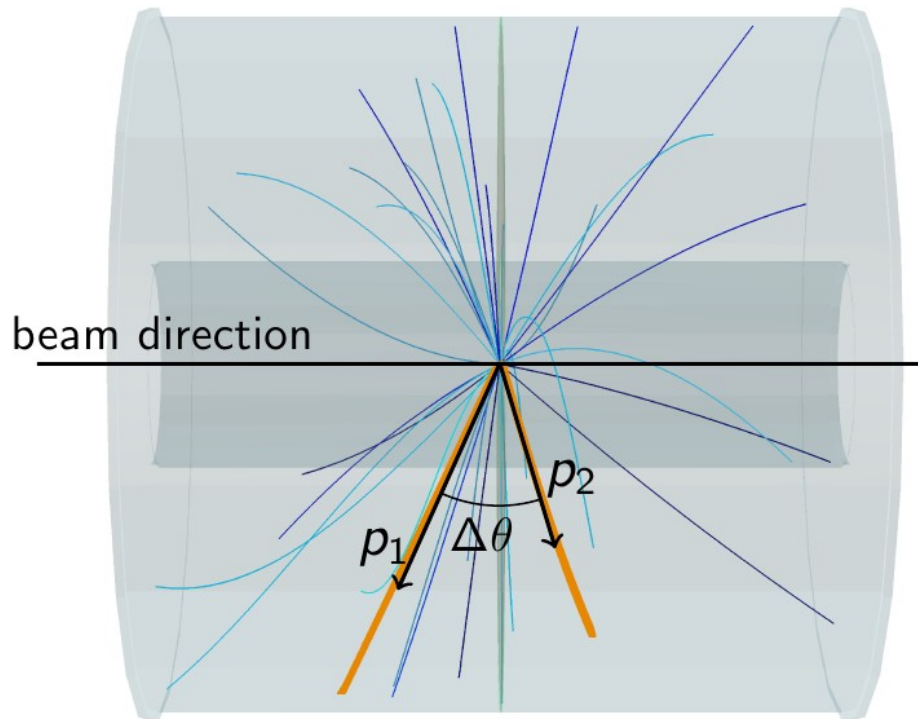
BFKLex simulations — pp

partonic min pT = 5 GeV
minijet min pT = 10 GeV, R = 0.5



Back up

Two-particle $\Delta\eta\Delta\phi$ angular correlations

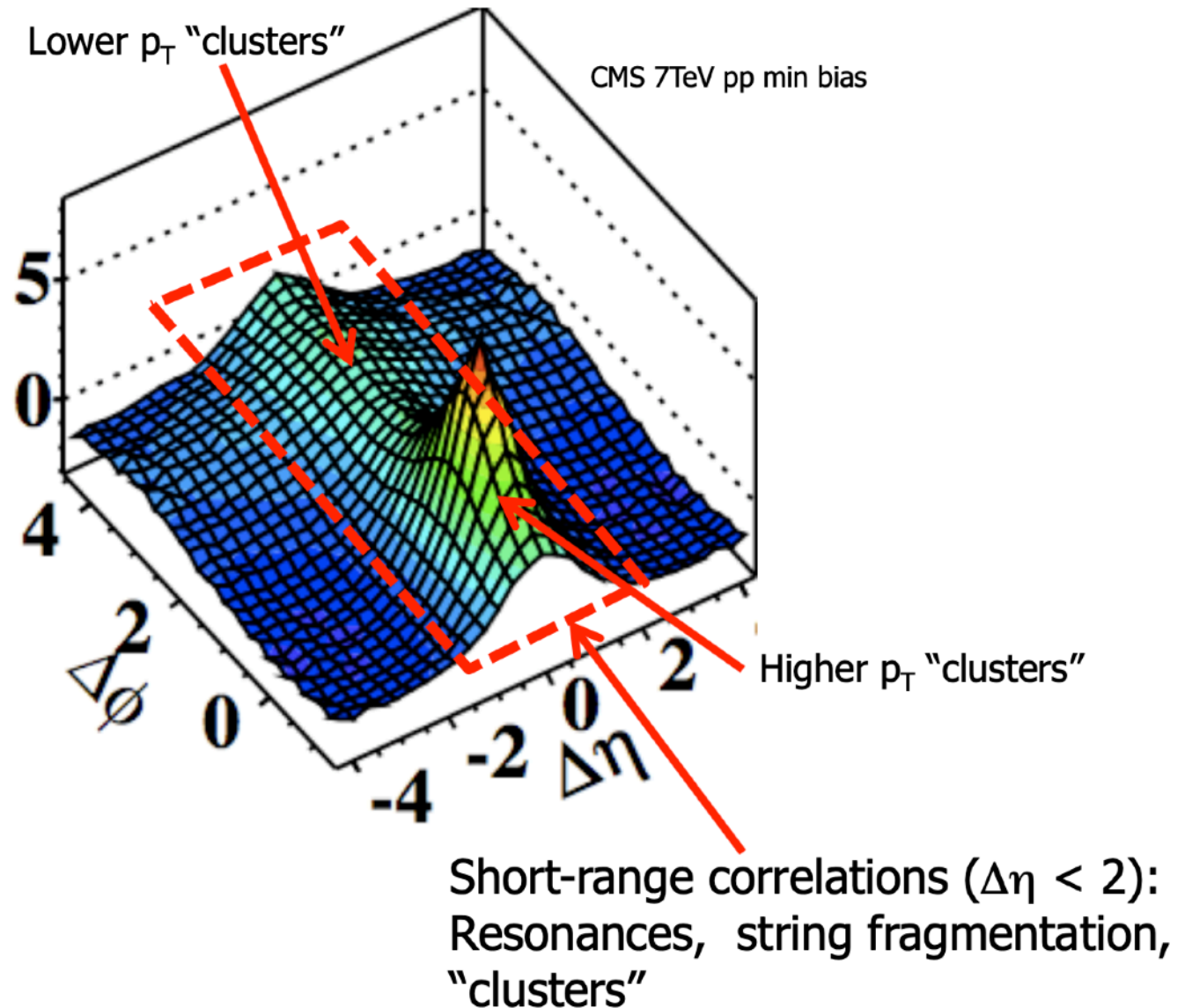


p - particle momentum;
 θ - polar angle;
 η - pseudorapidity:

$$\eta = -\ln \left| \operatorname{tg} \frac{\theta}{2} \right|$$

p_T - transverse momentum;
 φ - azimuthal angle;

Angular Correlation Functions

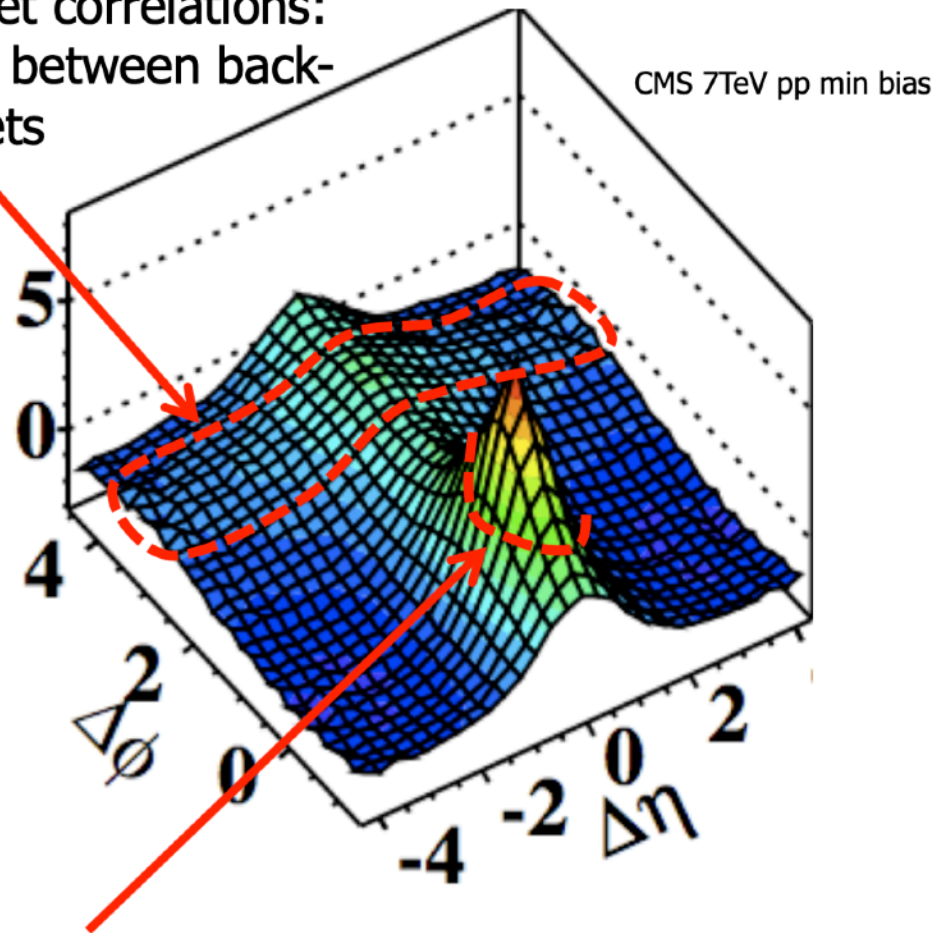




Angular Correlation Functions



“Away-side” ($\Delta\phi \sim \pi$) jet correlations:
Correlation of particles between back-
to-back jets



“Near-side” ($\Delta\phi \sim 0$) jet peak:
Correlation of particles
within a single jet